Annales Geophysicae (2004) 22: 3479–3501
SRef-ID: 1432-0576/ag/2004-22-3479

Annales Geophysicae

F-region ionospheric perturbations in the low-latitude ionosphere during the geomagnetic storm of 25–27 August 1987

A. V. Pavlov[1], **S. Fukao**[2], **and S. Kawamura**[3]

[1]Inst. of Terrestrial Magnetism, Ionosphere and Radio-Wave Propag., Russian Academy of Science, Troitsk, 142 190, Russia
[2]Research Institute for Sustainable Humanosphere, Kyoto University, Uji, Kyoto 611-0011, Japan
[3]National Institute of Information and Communications Technology, 4-2-1, Nukui-kita, Koganei, Tokyo 184-8795, Japan

Received: 10 February 2004 – Revised: 8 June 2004 – Accepted: 2 July 2004 – Published: 3 November 2004

Abstract. We have presented a comparison between the modeled $NmF2$ and $hmF2$, and $NmF2$ and $hmF2$ which were observed at the equatorial anomaly crest and close to the geomagnetic equator simultaneously by the Akita, Kokubunji, Yamagawa, Okinawa, Manila, Vanimo, and Darwin ionospheric sounders and by the middle and upper atmosphere (MU) radar (34.85° N, 136.10° E) during the 25–27 August 1987 geomagnetically storm-time period at low solar activity near 201°, geomagnetic longitude. A comparison between the electron and ion temperatures measured by the MU radar and those produced by the model of the ionosphere and plasmasphere is presented. The corrections of the storm-time zonal electric field, E_Λ, from 16:30 UT to 21:00 UT on 25 August bring the modeled and measured $hmF2$ into reasonable agreement. In both hemispheres, the meridional neutral wind, W, taken from the HWW90 wind model and the NRLMSISE-00 neutral temperature, T_n, and densities are corrected so that the model results agree with the ionospheric sounders and MU radar observations. The geomagnetic latitude variations in $NmF2$ on 26 August differ significantly from those on 25 and 27 August. The equatorial plasma fountain undergoes significant inhibition on 26 August. This suppression of the equatorial anomaly on 26 August is not due to a reduction in the meridional component of the plasma drift perpendicular to the geomagnetic field direction, but is due to the action of storm-time changes in neutral winds and densities on the plasma fountain process. The asymmetry in W determines most of the north-south asymmetry in $hmF2$ and $NmF2$ on 25 and 27 August between about 01:00–01:30 UT and about 14:00 UT when the equatorial anomaly exists in the ionosphere, while asymmetries in W, T_n, and neutral densities relative to the geomagnetic equator are responsible for the north-south asymmetry in $NmF2$ and $hmF2$ on 26 August. A theory of the primary mechanisms causing the morning and evening peaks in the electron temperature, T_e, is developed. An appearance, magnitude variations, latitude variations, and a disappearance of the morning T_e peaks during 25–27 August are caused by variations in E_Λ, thermospheric composition, T_n, and W. The magnitude of the evening T_e peak and its time location are decreased with the lowering of the geomagnetic latitude due to the weakening of the effect of the plasma drift caused by W on the electron density. The difference between 25 August and 26–27 August in an appearance, magnitude and latitude variations, and a disappearance of the evening T_e peak is caused by variations in W, the thermospheric composition, T_n, and E_Λ.

Key words. Ionosphere (Equatorial ionosphere; electric fields and currents; plasma temperature and density; ionospheric disturbances)

Correspondence to: A. V. Pavlov
(pavlov@izmiran.rssi.ru)

1 Introduction

The ionosphere at the geomagnetic equator and low geomagnetic latitudes is the site of important ionospheric phenomena, which include the equatorial electrojet, equatorial plasma fountain, equatorial (Appleton) anomaly, additional layers, plasma bubbles, and spread F. These low-latitude characteristic properties of the ionosphere have been studied observationally and theoretically for many years (Moffett, 1979; Anderson, 1981; Walker, 1981; Abdu et al., 1991; Bailey and Balan, 1996; Buonsanto, 1999; Rishbeth, 1975, 2000; Rishbeth and Fukao, 1995; Abdu, 1997, 2001).

A variety of global processes in the ionosphere/thermosphere/magnetosphere system is generated during geomagnetic storms, and magnetic storm effects on the neutral atmosphere and ionosphere depend on season, latitude, and longitude, as well as on the severity, time of occurrence, and duration of the storm (Buonsanto, 1999). The electron number density, N_e, can be decreased or increased in association with a magnetic storm in comparison with a quiet time N_e. In general, the equatorial anomaly is less developed during geomagnetic storm-time periods in com-

parison with the quiet time periods, however, enhancements of the equatorial anomaly have also been reported (Rishbeth, 1975). The geomagnetic storm changes in electric fields, thermospheric winds and neutral composition have been suggested as physical mechanisms to explain the variations in the low-latitude ionosphere, and plasmasphere structure and dynamics (Moffett, 1979; Anderson, 1981; Abdu et al., 1991; Buonsanto, 1999; Rishbeth, 1975, 2000; Rishbeth and Fukao, 1995; Abdu, 1997, 2001).

Geomagnetic storm processes, such as particle precipitation and Joule dissipation, lead to thermospheric heating and, as a result, to gravity waves/TIDs, disturbed thermospheric winds, and composition changes which reach low-latitude regions with a delay of a few hours from the geomagnetic storm onset. These perturbation neutral winds produce a part of storm-time changes in the equatorial electric fields through the ionospheric disturbance dynamo (Blanc and Richmond, 1980), while the other part of the storm-time equatorial electric field changes is produced by the solar wind-magnetosphere dynamo (Senior and Blanc, 1984; Spiro et al., 1988). The duration of electric field disturbances varies from tens of minutes to hours (Abdu et al., 1991). In general, the low-latitude electric fields undergo large departures from their quiet time averages during geomagnetic storms (Fejer and Scherliess, 1997; Fejer, 2002 and references therein). There are clear indications that a dawn-to-dusk disturbed electric field (i.e. eastward/westward on the day/night sides), penetrated in the equatorial ionosphere, is associated with a southward turning of the interplanetary magnetic field component, B_z (Abdu et al., 1991; Abdu, 1997). The intensity and duration of the disturbance electric field is controlled by many factors, such as the time constants of the decay/formation of the shielding charges in the inner magnetosphere, and auroral conductivity (Vasyliunas, 1975; Kelley et al., 1979; Gonzales et al., 1983), and, as a result, there are still questions concerning the prediction of the storm-time dependence of ionospheric electric fields (Fejer, 2002).

The storm-time F-region changes in the low-latitude ionosphere have been identified from F-layer height and frequency responses observed by ionosondes (see Abdu, 1997 and references therein). The incoherent scatter radar technique has expanded the range of information obtainable from the low-latitude sounders during geomagnetic storms. The dynamics of the low-latitude ionosphere was observed by the MU radar during the great geomagnetic storms of 6–8 February 1986, 20–21 January 1989, and 20–23 October 1989 (Oliver et al., 1988, 1991; Reddy et al., 1990). The changes of F-layer electron density observed by the MU radar in the 6–8 February 1986 storm were explained by changes in an influx of ionization from the plasmasphere, modulated by the passage of a large-scale southward traveling gravity wave (Oliver et al., 1988). In the 20–21 January 1989 storm, the observed large changes in the $F2$ region peak altitude from 23:00 LT to 02:40 LT were attributed to a large eastward electric field originating at auroral latitudes (Reddy et al., 1990). During the 20–23 October 1989 storm-time period, the first significant auroral display over Japan since 1960 was observed, and drastically different electron densities were discovered using the four radar beams, separated by about 250 km horizontally in the F-region (Oliver et al., 1991). The Arecibo radar observations of the ionospheric F-region during the 1–5 May 1995 geomagnetic storm period have shown the possible existance of a poleward expansion of the equatorial anomaly zone with the northern anomaly crest location close to 29° dip latitude (Buonsanto, 1999). Another anomalous low-latitude ionospheric feature was observed during 17–18 February 1999 highly disturbed geomagnetic period, when the Arecibo radar has recorded an anomalous nighttime ionospheric enhancement in which the nighttime value of the $F2$ peak electron density exceeded $10^6\,\mathrm{cm}^{-3}$ and the $F2$ peak altitude went above 400 km (Aponte et al., 2000).

The difficulties in theoretical studies of the response of the low-latitude ionosphere and plasmasphere to geomagnetic storms arise due to many competing processes imbedded in the production, loss and transport electrons and ions. The earlier simplified theoretical computations (Burge et al., 1973; Chandra and Spencer, 1976) have speculated on the importance of the disturbed neutral winds to the low-latitude ionospheric response to geomagnetic storms, but lack of data and/or model winds has hampered progress. Fesen et al. (1989) studied ionospheric effects in the low-latitude ionosphere during the 22 March 1979 geomagnetic storm period using the model without H^+ ions, ignoring electric field perturbations due to the storm, and suggesting that the temperatures of electron and ions are equal to the neutral temperature. It follows from the results of Fesen et al. (1989) that the equatorial anomaly may be disrupted by the magnetic storm, and the major factor influencing the storm-time ionospheric behavior is the neutral wind. This point of view was reiterated in recent studies, for example, by Sastri et al. (2000), with particular reference to the well–known storm in early November 1993. The coupled thermosphere ionosphere plasmasphere electrodynamic model was used by Fuller-Rowell et al. (2002) to model the low-latitude ionosphere and plasmasphere for a hypothetical geomagnetic storm at equinox and high solar activity without taking into account geomagnetic storm disturbances in an electric field. Their model results showed response features of the thermosphere and ionosphere as a unique system. In particular, Fuller-Rowell et al. (2002) found an equatorial response within 2 h of the storm onset and made clear the difference between the effects of meridional and zonal winds on the disturbed ionosphere.

As far as we know, there are no published comparisons between measurements and theoretical calculations of the low-latitude F-region electron density and temperature during geomagnetic storms, which would take into account the storm-time changes in the thermospheric wind, the electric field, the neutral composition, and the neutral temperature. In this paper, we present the first study of the complex problem of the low-latitude ionospheric response to the disturbed thermospheric wind, electric field, neutral composition, and neutral temperature.

It follows from the above-mentioned studies that horizontal neutral winds cause significant variations in the structure and dynamics of the low-latitude ionosphere and plasmasphere during geomagnetic storms. In the present work, we continue to investigate the role of horizontal neutral winds in the ionization distribution, plasma dynamics, structuring, and thermal balance of the low-latitude ionosphere in the present case study, in which $NmF2$ and $hmF2$ are observed simultaneously close to the same geomagnetic meridian at the geomagnetic longitudes of $201^\circ \pm 11^\circ$ by the Akita, Kokubunji, Yamagawa, Okinawa, Manila, Vanimo, and Darwin ionospheric sounders and by the middle and upper atmosphere (MU) radar at Shigaraki (34.85° N, 136.10° E, Japan) during the 25–27 August 1987 geomagnetically storm-time period at solar minimum.

The low-latitude ionosphere undergoes changes as a result of storm-time variations in plasma motion perpendicular to the geomagnetic field, $\boldsymbol{B}$, direction due to an electric field, $\boldsymbol{E}$, which is generated in the E-region. This electric field affects F-region plasma, causing both ions and electrons to drift in the same direction with a drift velocity, $\boldsymbol{V}^E = \boldsymbol{E} \times \boldsymbol{B} / B^2$. The zonal component of $\boldsymbol{V}^E$ (geomagnetic east-geomagnetic west component) is thought to have only a negligible effect on the low-latitude plasma densities (Anderson, 1981), and changes in the meridional component (component in the plane of a geomagnetic meridian) of the $\boldsymbol{E} \times \boldsymbol{B}$ drift velocity, caused by changes in the zonal electric field, affect the distribution of plasma in the low-latitude ionospheric F-region. During geomagnetic storms, the vertical equatorial drift shows significant variability in the magnitude (Fejer, 2002), and, as a result, the vertical drift given by the empirical model of Fejer and Scherliess (1997) for the geomagnetically storm-time periods is the averaged vertical drift and can differ from the vertical drift for the studied geomagnetically disturbed time period. The examination of the model of the meridional component of the drift velocity has been driven by the relationship between the zonal electric field and the dynamics of the $F2$-layer close to the geomagnetic equator. The present work studies the relationship between the zonal electric field and the dynamics of the low-latitude $F2$-layer in the low-latitude ionosphere, when $NmF2$ and $hmF2$ are observed simultaneously close to the same geomagnetic meridian by the Akita, Kokubunji, Yamagawa, Okinawa, Manila, Vanimo, and Darwin ionospheric sounders and by the MU radar during the 25–27 August 1987 geomagnetically storm-time period.

Many theoretical models of the plasmasphere and low-latitude ionosphere were constructed and have been applied to study a wide variety of equatorial ionosphere characteristic properties during geomagnetically quiet conditions (see Moffett, 1979; Anderson, 1981; Walker, 1981; Bailey and Balan, 1996; Rishbeth, 2000; Abdu, 1997, 2001, and references therein). In the present work, we investigate the equatorial anomaly geomagnetic storm characteristics (the equatorial trough, and crest latitudes and magnitudes) from the comparison between the measured and modeled N_e and electron temperatures, T_e, during 25–27 August 1987 using the new two-dimensional time dependent model of the low- and middle-latitude plasmasphere and ionosphere (Pavlov, 2003), which employs the updated rate coefficients of chemical reactions of ions and the updated N_2, O_2, and O photoionization and photoabsorption cross sections. Ionospheric models are particularly valuable for investigating the changes that would result, in observed quantities, from changes in individual input parameters, and, therefore, the theoretical study of the ionospheric storm response features is a highly complex task in the absence of the measurements of the disturbed thermospheric wind, electric field, neutral composition, and neutral temperature for the studied time period at low-latitudes close to 201° geomagnetic longitude. Nevertheless, it is possible to evaluate whether or not the storm-time variations of the main ionospheric parameters measured by the ionospheric sounders and the MU radar are consistent with what is calculated from the model of the ionosphere and plasmasphere. The model of the ionosphere and plasmasphere of Pavlov (2003) uses the NRLMSISE-00 neutral temperature and density model (Picone et al., 2002) and the HWW90 neutral wind model (Hedin et al., 1991) as the model input parameters. As a result, model/data discrepancies can arise due to the possible inability of the neutral atmosphere and wind models to accurately predict the storm-time thermospheric response to the studied time period in the upper atmosphere. We investigate how well the MU radar data and the Akita, Kokubunji, Yamagawa, Okinawa, Manila, Vanimo, and Darwin ionospheric sounder measurements of electron densities taken during 25–27 August 1987 agree with those calculated by the model of the ionosphere and plasmasphere.

The horizontal neutral wind drives the low-latitude F-layer plasma along magnetic field lines and causes significant north–south asymmetry in the equatorial ionization anomaly during geomagnetically quiet conditions (Balan and Bailey, 1995; Balan et al., 1997 a,b). As far as the authors know, our investigation is the first theoretical study of the role of variations in the neutral winds, temperature, and densities in producing the north−south asymmetry in the storm-time electron density.

Otsuka et al. (1998) found that the occurrence and strength of the morning and evening peaks in T_e over the MU radar depend on altitude, season, and solar activity under magnetically quiet conditions during 1986–1995. Pavlov et al. (2004) studied, for the first time, the latitude dependence of the occurrence and strength of the morning and evening peaks in T_e and the mechanisms causing these peaks in the low-latitude ionosphere during geomagnetically quiet-time conditions of 19–21 March 1988. In this work, we report the first results obtained from a study of the latitude dependence of the occurrence and strength of the morning and evening peaks in T_e and the mechanisms causing these peaks in the low-latitude ionosphere during the 25–27 August 1987 geomagnetically storm-time period. The reliability of the conclusions is based on the comparison between the measured MU radar and modeled T_e, and the use of the updated electron cooling rates (Pavlov, 1998a, b; Pavlov and Berrington, 1999) in the model.

2 Theoretical model

The model of the low- and middle latitude ionosphere and plasmasphere, which is described in detail by Pavlov (2003), calculates number densities, N_i, of $O^+(^4S)$, H^+, NO^+, O_2^+, N_2^+, $O^+(^2D)$, $O^+(^2P)$, $O^+(^4P)$, and $O^+(^2P^*)$ ions, N_e, T_e, and T_i. As the model inputs, the horizontal components of the neutral wind are specified using the HWW90 wind model (Hedin et al., 1991), the model solar EUV fluxes are taken from the EUVAC model (Richards et al., 1994), while neutral densities and temperature are taken from the NRLMSISE-00 model (Picone et al., 2002).

The model calculations are carried out in dipole orthogonal curvilinear coordinates q, U, and Λ, where q is aligned with, and U and Λ are perpendicular to $\boldsymbol{B}$, and the U and Λ coordinates are constant along a dipole magnetic field line. It should be noted that $q=(R_E/R)^2 \cos\Theta$, $U=(R_E/R)\sin^2\Theta$, and the value of Λ is the geomagnetic longitude where R is the radial distance from the Earth's center, $\Theta=90^0-\varphi$ is the geomagnetic colatitude, φ is the geomagnetic latitude, R_E is the Earth's radius. The McIlwain parameter $L=R/(R_E \sin^2\Theta)$ can be presented as $L=U^{-1}$.

The model takes into account that the $\boldsymbol{E}\times\boldsymbol{B}$ plasma drift velocity can be presented as $\boldsymbol{V}^E=V_\Lambda^E\boldsymbol{e}_\Lambda+V_U^E\boldsymbol{e}_U$, where $V_\Lambda^E=E_U/B$ is the zonal component of $\boldsymbol{V}^E$, $V_U^E=-E_\Lambda/B$ is the meridional component of $\boldsymbol{V}^E$, $\boldsymbol{E}=E_\Lambda\boldsymbol{e}_\Lambda+E_U\boldsymbol{e}_U$, E_Λ is the Λ (zonal) electric field in the dipole coordinate system, E_U is the U (meridional) component of $\boldsymbol{E}$ in the dipole coordinate system, $\boldsymbol{e}_\Lambda$ and $\boldsymbol{e}_U$ are unit vectors in Λ and U directions, respectively, $\boldsymbol{e}_U$ is directed downward at the geomagnetic equator.

The trajectory of the ionospheric plasma perpendicular to magnetic field lines and the moving coordinate system are determined from equations derived by Pavlov (2003). The effects of the zonal (geomagnetic east- geomagnetic west) component of the $\boldsymbol{E}\times\boldsymbol{B}$ drift on N_e, N_i, T_e, and T_i are not taken into consideration because it is believed (Anderson, 1981) that these effects are negligible. As a result, the model works as a time dependent two-dimensional (q and U coordinates) model of the ionosphere and plasmasphere. In this approximation, the trajectory of the ionospheric plasma in the U direction is found from the equation as (Pavlov, 2003)

$$\frac{\partial}{\partial t}U = -E_\Lambda^{\rm eff} R_E^{-1} B_0^{-1}, \quad (1)$$

$$E_\Lambda^{\rm eff} = E_\Lambda h_\Lambda R_E^{-1}, \quad (2)$$

where $h_\Lambda = R\sin\Theta$, B_0 is the equatorial value of B for $R=R_E$ and $\Theta=0$.

The model takes into account that magnetic field lines are "frozen" to the $\boldsymbol{E}\times\boldsymbol{B}$ drift of the ionospheric and plasmaspheric plasma if (Pavlov, 2003)

$$\frac{\partial}{\partial q}(E_\Lambda^{\rm eff}) = 0, \quad (3)$$

i.e. the effective electric field, $E_\Lambda^{\rm eff}$, is not changed along magnetic field lines.

It should be noted that Eqs. (2) and (3) determine the changes in the zonal electric field along magnetic field lines, and the altitude dependence of this component of the electric field in the ionosphere and plasmasphere.

The time variations of the zonal electric field used in the model calculations during 25–27 August 1987 are presented in the middle and bottom panels of Fig. 1. The solid line in the bottom panel of Fig. 1 shows the empirical F-region storm-time equatorial zonal electric field found from the empirical model of the vertical drift velocity of Fejer and Scherliess (1997). For the time periods from 16:30 UT to 21:00 UT on 25 August, this empirical electric field is modified by the use of the comparison between the measured and modeled values of $hmF2$ over the Manila sounder (see Sect. 4.1). The resulting storm-time equatorial zonal electric field, E_Λ^{ES}, given by crosses in the bottom panel of Fig. 1, is used in the model calculations at the F-region altitudes over the geomagnetic equator. The top panel of Fig. 1 shows the measured (triangles) and modeled (solid line) F-region plasma vertical drift velocity over Jicamarca, which will be discussed in Sect. 4.1.

There are no MU radar vertical drift velocity measurements for the studied time period. We take into account that the perpendicular drifts over Arecibo and the MU radar are similar for the same local time (Takami et al., 1996). Therefore, for geomagnetically quiet conditions, it would be possible to use the Arecibo average quiet time zonal electric field, E_Λ^{AQ}, in model simulations at the F-region altitudes, 29° geomagnetic latitude, and 201° geomagnetic longitude. This zonal electric field is found from Fig. 2 of Fejer (1993) and is shown in the middle panel of Fig. 1 (dashed line). To find the disturbed zonal electric field, E_Λ^{AS}, at the F-region altitudes, 29° geomagnetic latitude, and 201° geomagnetic longitude, we find the difference, ΔE_Λ, between the disturbed (crosses in the bottom panel of Fig. 1) and geomagnetically quiet zonal electric fields over the geomagnetic equator. The F-region geomagnetically quiet equatorial zonal electric field is found from the empirical model of the vertical drift velocity of Scherliess and Fejer (1999) and is shown by the dashed line in the bottom panel of Fig. 1. In the absence of measurements and an empirical model of a storm-time zonal electric field for the studied time period at geomagnetic latitudes close to 29°, we suggest that the studied storm-time variations in the zonal electric field at the F-region altitudes are the same at the geomagnetic equator and at the geomagnetic latitude of 29°, i.e. $E_\Lambda^{AS}=E_\Lambda^{AQ}+\Delta E_\Lambda$. The value of E_Λ^{AS} found is shown by crosses in the middle panel of Fig. 1.

Equations (1)–(3) determine the trajectory of the ionospheric plasma perpendicular to magnetic field lines and the moving coordinate system. It follows from Eq. (1) that time variations of U caused by the existence of the zonal electric field are determined by time variations of $E_\Lambda^{\rm eff}$ given by Eq. (2). We have to take into account Eq. (3), which shows that $E_\Lambda^{\rm eff}$ is not changed along magnetic field lines. The equa-

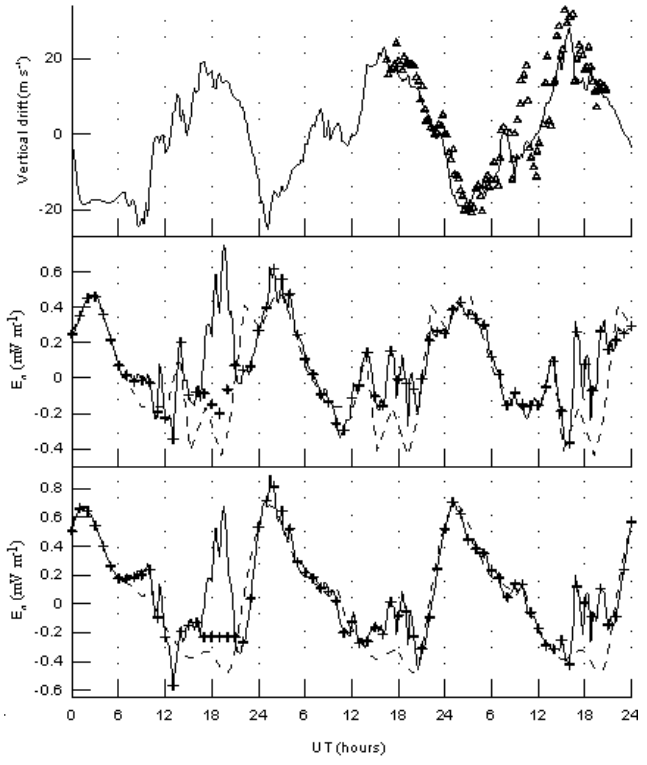

Fig. 1. The bottom and middle panels show diurnal variations of the zonal electric field during 25–27 August 1987. The solid line in the bottom panel shows the F-region storm-time equatorial zonal electric field found from the empirical model of Fejer and Scherliess (1997), while the F-region geomagnetically quiet equatorial zonal electric field found from the empirical model of Scherliess and Fejer (1999) is presented by the dashed line in the bottom panel. For the time periods from 16:30 UT to 21:00 UT on 25 August, the empirical electric field, given by the solid line in the bottom panel, is modified by use of the comparison between the measured and modeled values of $hmF2$ over the Manila sounder (see Sect. 4.1). The resulting storm-time equatorial zonal electric field, E_{Λ}^{ES}, given by crosses in the bottom panel of Fig. 1, is used in the model calculations at the F-region altitudes over the geomagnetic equator. The average quiet time value of the zonal electric field at the F-region altitudes over Arecibo (dashed line in the middle panel) is found from Fejer (1993). To find the disturbed zonal electric field, E_{Λ}^{AS}, at the F-region altitudes, 29° geomagnetic latitude, and 201° geomagnetic longitude, we find the difference, ΔE_{Λ}, between the disturbed (crosses in the bottom panel) and geomagnetically quiet (dashed line in the bottom panel) zonal electric field. We suggest that the studied storm-time variations in the zonal electric field at the F-region altitudes are the same at the geomagnetic equator and at 29° geomagnetic latitude, i.e. $E_{\Lambda}^{AS}=E_{\Lambda}^{AQ}+\Delta E_{\Lambda}$. The E_{Λ}^{AS} used is shown by crosses in the middle panel. The F-region plasma vertical drift velocity, measured by the Jicamarca, radar from 16:31 UT on 26 August 1987, to 20:45 UT on 27 August 1987, is displayed by triangles in the top panel, while the F-region plasma vertical drift velocity over Jicamarca calculated by the empirical model of Fejer and Scherliess (1997) for the time period of 25–27 August 1987 is shown by the solid line in the top panel.

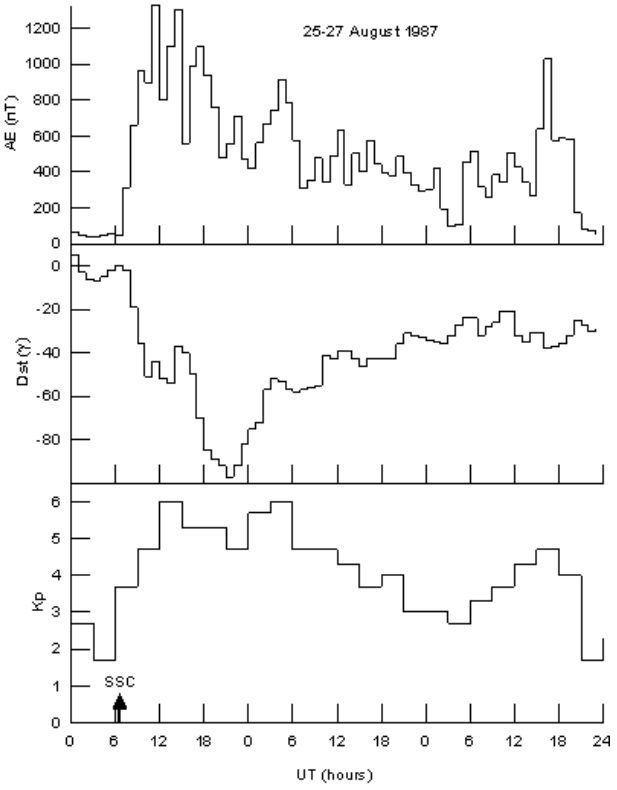

Fig. 2. The variation in the AE index (top panel), the D_{st} index (middle panel), and K_p index (bottom panel) during 25–27 August 1987. The SSC onset of the geomagnetic storm is shown by the arrow in the bottom panel.

torial and Arecibo values of the storm-time zonal electric field are used to find the equatorial and Arecibo values of $E_{\Lambda}^{\rm eff}$ from Eqs. (2) and (3). The equatorial value of $E_{\Lambda}^{\rm eff}$ is used for magnetic field lines with an apex altitude, $h_{ap}=R_{eq}-R_E$, less than 600 km, where R_{eq} is the equatorial radial distance of the magnetic field line from the Earth's center and R_E is the Earth's radius. The Arecibo value of $E_{\Lambda}^{\rm eff}$ is used if the apex altitude is greater than 2126 km. A linear interpolation of the equatorial and Arecibo values of $E_{\Lambda}^{\rm eff}$ is employed at intermediate apex altitudes.

The model calculates the values of N_i, N_e, T_i, and T_e in the fixed nodes of the fixed volume grid. This Eulerian computational grid consists of a distribution of the dipole magnetic field lines in the ionosphere and plasmasphere. One hundred dipole magnetic field lines are used in the model for each fixed value of Λ. The number of the fixed nodes taken along each magnetic field line is 191. For each fixed value of Λ, the region of study is a (q, U) plane, which is bounded by two dipole magnetic field lines. The low boundary magnetic field line has h_{ap}=150 km. The upper boundary magnetic field line has h_{ap}=4491 km and intersects the Earth's surface at two middle-latitude geomagnetic latitudes: ±40°. The computational grid dipole magnetic field lines are distributed between these two boundary lines. They have the interval, Δh_{ap}, of 20 km between h_{ap} of the low boundary

Table 1. Ionosonde station and radar names and locations.

Ionosonde station and radar names	Geographic latitude	Geographic longitude	Geomagnetic latitude	Geomagnetic longitude
Akita	39.7	140.1	29.6	206.2
Kokubunji	35.7	139.5	25.6	206.2
Yamagawa	31.2	130.6	20.5	198.6
Okinawa	26.3	127.8	15.4	196.3
Manila	14.6	121.1	3.4	190.6
Vanimo	−2.7	141.3	−12.4	211.9
Darwin	−12.4	130.9	−23.0	202.0
MU radar	34.9	136.1	24.5	203.2

line and h_p of the nearest computational grid dipole magnetic field line. The value of Δh_{ap} is increased from 20 km to 45 km linearly as we go from the low computational grid boundary line to the upper computational grid dipole magnetic field line. We expect our finite-difference algorithm, which is described below, to yield approximations to N_i, N_e, T_i, and T_e in the ionosphere and plasmasphere at discrete times t=0, Δt, 2Δt,... with the time step Δt=10 min. The model starts at 05:14 UT on 23 August. This UT corresponds to 14:00 solar local time, SLT, at the geomagnetic equator and 201° geomagnetic longitude (SLT=UT+ψ/15, where ψ is the geographic latitude). The model is run from 05:14 UT on 23 August 1987 to 24:00 UT on 24 August 1987 before model results are used.

3 Solar geophysical conditions and data

The storm period under study occurred at solar minimum when the 10.7 cm solar flux was between 85 and 90 during 25–27 August 1987, and the 3-month average of the 10.7 cm solar flux was 87. In Fig. 2 starting from the bottom panel, the geomagnetic activity indexes K_p, D_{st}, and AE, are plotted versus universal time, taken by Internet from the database of the National Geophysical Data Center (Boulder, Colorado).

Intense storms have minimum values of $D_{st} \leq -100$ nT (Gonzalez and Tsurutani, 1987), while the studied storm has the minimum value of $D_{st}=-97$ nT at 21:00 UT–22:00 UT on 25 August 1987 with the following recovery phase of the geomagnetic storm. Thus, this storm can be classified as a moderate storm which is very close to an intense storm. The D_{st} index remained at less than −50 nT up to 09:00 UT on 26 August while the AE index remained perturbed until 21:00 UT on 27 August. The SSC onset of the geomagnetic storm was at 06:58 UT on 25 August and is shown by the arrow in the bottom panel of Fig. 2. The K_p index reached its maximum value of 6_0 at 12:00 UT–15:00 UT on 25 August 1987 and at 03:00 UT–06:00 UT on 26 August 1987. The studied storm-time period was preceded by fairly quiet conditions when the value of the geomagnetic K_p index was between 0 and 3_0 for most of the time period of 18–24 August 1987, except between 09:00 UT and 15:00 UT on 24 August when the magnitude of K_p was 4_-.

The middle and upper atmosphere (MU) radar at Shigaraki, which is located at the geomagnetic latitude of 24.5° and the geomagnetic longitude of 203.2°, operated from 16:00 LT on 25 August to 14:00 LT on 27 August. The capabilities of the radar for incoherent scatter observations have been described and compared with those of other incoherent scatter radars by Sato et al. (1989) and Fukao et al. (1990). Rishbeth and Fukao (1995) reviewed the MU radar studies of the ionosphere and thermosphere. The data that we use in this work are the measured time variations of altitude profiles of the electron density and temperature, and the ion temperature between 200 km and 600 km over the MU radar.

We use hourly critical frequencies, $foF2$ and foE, of the $F2$ and E-layers, and maximum usable frequency parameter, M(3000)$F2$, data from the Akita, Kokubunji, Yamagawa, Okinawa, Manila, Vanimo, and Darwin ionospheric sounder stations available at the Ionospheric Digital Database of the National Geophysical Data Center, Boulder, Colorado. The locations of these ionospheric sounder stations and the location of the MU radar are shown in Table 1. The values of the peak density, $NmF2$, of the $F2$ layer are related to the critical frequency $foF2$ as $NmF2=1.24\cdot10^{10}\ foF2^2$, where the unit of $NmF2$ is m^{-3}, the unit of $foF2$ is MHz. In the absence of adequate $hmF2$ data, we use the relation between $hmF2$ and the values of M(3000)$F2$, $foF2$, and foE recommended by Dudeney (1983) from the comparison of different approaches as $hmF2=1490/[M(3000)F2+\Delta M]-176$, where $\Delta M=0.253/(foF2/foE-1.215)-0.012$. There are no foE data in the Ionospheric Digital Database for the 25–27 August 1987 time period for the Manila ionosonde station, and we are forced to use ΔM=0, i.e. the $hmF2$ formula of Shimazaki (1955) is used for the Manila ionosonde station data. The sounders and the MU radar are within ±11° geomagnetic longitude of one another. As a result, the model simulations are carried out in the plane of 201° geomagnetic longitude to compare the model results with the MU radar and sounder measurements.

4 Results

4.1 Zonal electric field corrections from the observed variations in $hmF2$

The measured (squares) and calculated (lines) $NmF2$ (bottom panel) and $hmF2$ (top panel) are displayed in Fig. 3 for the 25–26 August 1987 time period above the Vanimo (two bottom panels), Manila (two middle panels), and Okinawa (two top panels) ionosonde stations. The solid lines in Fig. 3 show the calculated $NmF2$ and $hmF2$ over Manila using the corrected storm-time (crosses in the bottom and middle panels of Fig. 1), while the dotted lines in Fig. 3 are $NmF2$ and $hmF2$ from the model with an uncorrected (solid lines in the bottom and middle panels of Fig. 1) zonal electric field. The dashed lines will be explained later in this section. The original HWW90 wind and NRLMSISE-00 neutral temperature and densities are used in the model calculations.

There are no foE data for the 25–27 August 1987 time period for the Manila ionosonde station, and we believe that $hmF2$=1490/M(3000)$F2$ over Manila (see Sect. 3). It means that the real values of $hmF2$ are less than those shown in the middle panel of Fig. 3 by squares. As a result, if the modeled $hmF2$ is less than the measured $hmF2$, then we cannot derive conclusions about errors of the model calculations. For example, there is the disagreement between the measured and modeled $hmF2$ over Manila from about 01:00 UT to about 09:00 UT on 25 August. However, we have no right to correct the model input parameters in order for the measured and modeled $hmF2$ to agree, because this disagreement (or a part of this disagreement) can be explained by errors in $hmF2$ found only from the M(3000)$F2$ measurements.

The comparison between the measured $hmF2$ (squares) and the calculated results, shown by the dotted lines in Fig. 3, clearly indicates that there is a disagreement between the measured and modeled $hmF2$ from about 17:00 UT to about 21:00 UT on 25 August, if the equatorial upward $\boldsymbol{E}\times\boldsymbol{B}$ drift given by Fejer and Scherliess (1997) is used. As was pointed out above, the measured $hmF2$ are less than those shown in the middle panel of Fig. 3 by squares. On the other hand, the measured $hmF2$ is less than the calculated $hmF2$ over Manila, and we conclude that this disagreement is explained by errors of the model calculations. The model simulations show that changes in the NRLMSISE-00 neutral temperature and densities do not lead to considerable variations in $hmF2$ and cannot bring the measured and modeled $hmF2$ into agreement. By comparing the measured and calculated $hmF2$ over Manila, we found that the required equatorial upward $\boldsymbol{E}\times\boldsymbol{B}$ drift is weaker during the time period from 16:30 UT to 21:00 UT on 25 August than that given by Fejer and Scherliess (1997). The use of the corrected storm-time model equatorial zonal electric field found, shown by crosses in Fig. 1, brings into agreement the measured (squares) and modeled (solid lines) $hmF2$ shown in Fig. 3.

The weakening of the zonal electric field from 16:30 UT to 21:00 UT on 25 August causes a noticeable decrease in $hmF2$ over Manila. The equatorial plasma drift model of

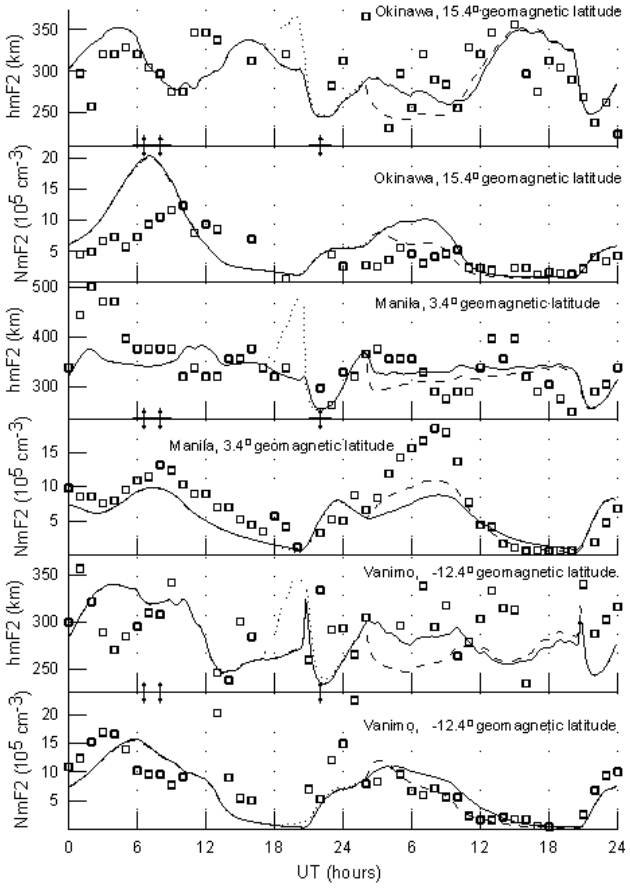

Fig. 3. Observed (squares) and calculated (lines) $NmF2$ and $hmF2$ during 25–26 August 1987 over the Vanimo (two bottom panels), Manila (two middle panels), and Okinawa (two top panels), The solid lines show the calculated $NmF2$ and $hmF2$ using the storm-time corrected (crosses in the bottom and middle panels of Fig. 1) zonal electric field, while the dotted lines are $NmF2$ and $hmF2$ from the model with the uncorrected (solid lines in the bottom and middle panels of Fig. 1) zonal electric field. To produce the model results shown by the dashed lines, the storm-time corrected zonal electric field shown by crosses in the middle and bottom panels of Fig. 1 was divided by a factor of 10 at all the studied geomagnetic latitudes from 02:00 UT to 10:00 UT on 26 August 1987. The original HWW90 wind and NRLMSISE-00 neutral temperature and densities are used in the model calculations. The start times of the sudden commencement (06:58 UT on 25 August), main phase (08:00 UT on 25 August) and recovery phase (22:00 UT on 25 August) of the geomagnetic storm are indicated by the arrows.

Fejer and Scherliess (1997) does not reproduce this weakening in the zonal electric field which follows from the Manila ionosonde station measurements, because this plasma drift model produces only the averaged vertical drift and this vertical drift, can differ from the vertical drift for the studied geomagnetically disturbed time period. This conclusion is supported by the top panel of Fig. 1, where triangles display the F-region plasma vertical drift velocity measured by the Jicamarca radar from 16:31 UT on 26 August 1987 to 20:45 UT on 27 August 1987, while the F-region plasma vertical drift

velocity over Jicamarca, given by the empirical model of Fejer and Scherliess (1997) for the time period of 25–27 August 1987, is shown by the solid line. We conclude from the top panel of Fig. 1 that the measured drift is very variable, and the difference between the empirical model drift velocity and the measured drift velocity during some short time periods on 27 August is comparable to the magnitude of the abovementioned weakening in the electric field on 25 August.

If $E_\Lambda > 0$, then a decrease in E_Λ leads to a slower plasma motion from low to high geomagnetic latitudes perpendicular to $\boldsymbol{B}$, causing an increase in $NmF2$ and a decrease in $hmF2$ close to the geomagnetic equator, i.e. it is possible that the disagreement between the measured and modeled $NmF2$ over Manila on 26 August (see middle panel of Fig. 3) could be eliminated by a weakening of E_Λ on 26 August in comparison with that shown by crosses in the middle and bottom panels of Fig. 1. To test this hypothesis, the value of E_Λ shown by crosses in the middle and bottom panels of Fig. 1 was divided by a factor of 10 at all the studied geomagnetic latitudes from 02:00 UT to 10:00 UT on 26 August. It follows from the model results shown by dashed lines in Fig. 3 that this weakening in E_Λ causes an increase in $NmF2$ from about 02:00 UT to about 11:00 UT and a decrease in $hmF2$ from about 02:00 UT to about 22:00 UT on 26 August over Manila. However, only a small part of the disagreement between the measured and modeled $NmF2$ over Manila can be explained by this reduction in E_Λ. Furthermore, the suggested weakening in E_Λ brings the measured and modeled $hmF2$ into disagreement over Vanimo and Okinawa on 26 August and worsens the agreement between the measured and modeled $hmF2$ over Manila from about 03:00 UT to 07:00 UT and from about 13:00 UT to about 15:00 UT on 26 August. As a result, we have no arguments to correct E_Λ from the comparison between the measured and modeled $hmF2$ and $NmF2$ on 26 August. We show in Sect. 4.2 that the model/data discrepancies over Manila arise due to an inability of the NRLMSISE-00 model to accurately predict the thermospheric response to the studied time period in the upper atmosphere.

4.2 Diurnal variations of $NmF2$, $hmF2$, T_e and T_i

The measured (squares) and calculated (lines) $NmF2$ and $hmF2$ are displayed in the two lower panels of Figs. 4–9 for the 25–27 August 1987 time period above the Darwin (Fig. 4), Vanimo (Fig. 5), Manila (Fig. 6), Okinawa (Fig. 7), Yamagawa (Fig. 8), and Akita (Fig. 9) ionosonde stations, while the modeled electron and O^+ ion temperatures at the $F2$-region main peak altitude above the ionosonde stations are presented in the two upper panels of these figures. Figure 10 shows the measured (crosses) and calculated (lines) $NmF2$ (bottom panel) and electron (middle panel) and O^+ ion (top panel) temperatures at $hmF2$ above the MU radar. Squares in the two lower panels of Fig. 10 show the measured $NmF2$ and $hmF2$ during 25–27 August 1987 above the Kokubunji ionosonde station. The latitude and longitude location of the Kokubunji sounder is very close to that of the MU radar and the calculated $hmF2$, N_e, T_e, and T_i above this sounder are practically the same as those in Fig. 10. The results obtained from the model of the ionosphere and plasmasphere using the combination of E_Λ^{eff} based on the uncorrected zonal disturbed electric field (given by the solid lines in the bottom and middle panel of Fig. 1), the NRLMSISE-00 neutral temperature and densities, and the HWW90 wind as the input model parameters are shown by the dotted lines in Figs. 4–10. The solid lines in Figs. 4–10 show the results given by the model with the corrected zonal electric field (given by crosses in the bottom and middle panel of Fig. 1), the corrected NRLMSISE-00 neutral temperature and densities, and the corrected neutral HWW90 wind. Dashed lines in Figs. 4–10 show the results from the model with the same corrections of the NRLMSISE-00 [O] and meridional neutral HWW90 wind as for solid lines and when the value of E_Λ^{eff} used in producing results shown by solid lines (based on the corrected zonal electric field given by crosses in the bottom and middle panel of Fig. 1) was divided by a factor of 10 at all the studied geomagnetic latitudes. The NRLMSISE-00 and HWW90 model corrections will be explained below in this section.

It follows from Figs. 4–10 that we are not capable of making the measured (squares and crosses) and modeled (dotted lines) $NmF2$, $hmF2$, T_e, and T_i agree if the NRLMSISE-00 neutral temperature and densities, the HWW90 wind, the uncorrected E_Λ^{eff} (based on the zonal electric field given by the solid lines in the bottom and middle panel of Fig. 1) are used as the input model parameters. A part of these disagreements between the measured and modeled N_e, T_e, and T_i is probably due to inaccuracies in the model inputs, such as a possible inability of the NRLMSIS-00 neutral temperature and densities model, the HWW90 wind model, and the empirical electric field model of Fejer and Scherliess (1997) to accurately predict the neutral densities, temperature, wind components, and zonal electric field for the studied period. These models can be corrected for the studied time period from the comparisons between the measured and modeled N_e, T_e, and T_i.

By comparing the dotted lines and crosses in the top panel of Fig. 10, it is seen that the measured ion temperature is higher than the calculated one. It follows from Fig. 10 that there is an agreement between the measured and modeled electron temperature at $hmF2$ over the MU radar from 16:00 UT on 25 August 1987 to 11:00 UT on 26 August 1987. As a result, we can infer that the disagreement between the measured and modeled ion temperature is caused by inaccuracies in the NRLMSISE-00 model prediction of the neutral temperature, T_n, for the studied geomagnetic storm-time period. To overcome the disagreement between the measured and modeled ion temperature, we multiply the value of T_n by the correction factor, C, which is determined as

$$\begin{aligned} &C = 1.2 + 0.2\cdot\sin[(\text{UT}-21)\cdot\pi/12] \text{ from} \\ &15:00 \text{ UT on 25 August to } 15:00 \text{ UT on 26 August,} \\ &C = 1.1 + 0.1\cdot\sin[(\text{UT}-21)\cdot\pi/12] \text{ from} \\ &15:00 \text{ UT on 26 August to } 15:00 \text{ UT on 27 August,} \end{aligned} \quad (4)$$

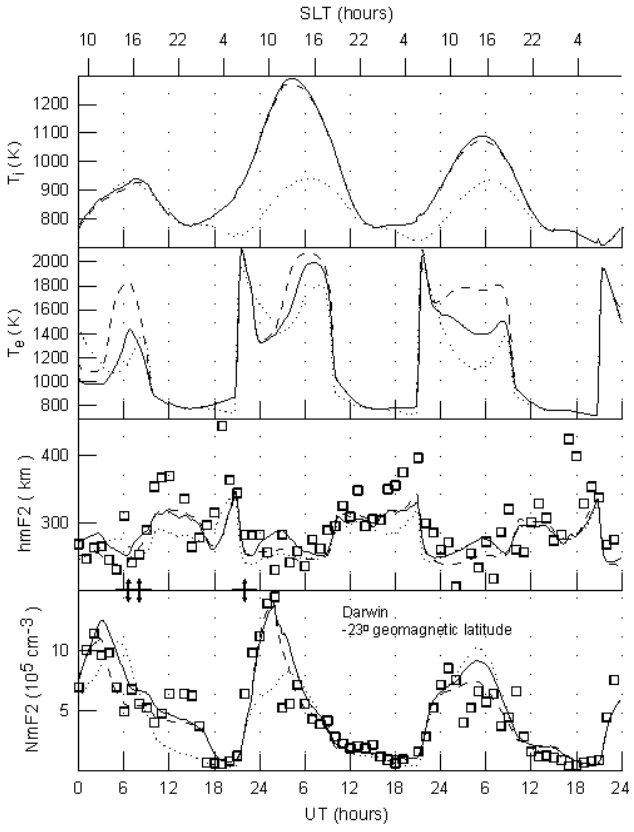

Fig. 4. Observed (squares) and calculated (lines) $NmF2$ and $hmF2$ (two lower panels), and electron and O^+ ion temperatures (two upper panels) at the $F2$-region main peak altitude above the Darwin ionosonde station during 25–27 August 1987. SLT is the solar local time at the Darwin ionosonde station. The results obtained from the model of the ionosphere and plasmasphere, using E_Λ^{eff} based on the uncorrected zonal electric field, given by the solid lines in Fig. 1, the NRLMSISE-00 neutral temperature and densities, and the HWW90 wind as the input model parameters, are shown by dotted lines. Solid lines show the results obtained from the model of the ionosphere and plasmasphere using the combinations of E_Λ^{eff} based on the corrected zonal electric field given by crosses in Fig. 1, the corrected NRLMSISE-00 neutral temperature and densities, and the corrected meridional HWW90 wind. Dashed lines show the results from the model with the same corrections of the NRLMSISE-00 [O] and meridional HWW90 wind as for solid lines and when the value of E_Λ^{eff} used in producing results shown by solid lines (based on the corrected zonal electric field given by crosses in the bottom and middle panel of Fig. 1) was divided by a factor of 10 at all the studied geomagnetic latitudes during the studied time period. The start times of the sudden commencement (06:58 UT on 25 August), main phase (08:00 UT on 25 August) and recovery phase (22:00 UT on 25 August) of the geomagnetic storm are indicated by the arrows.

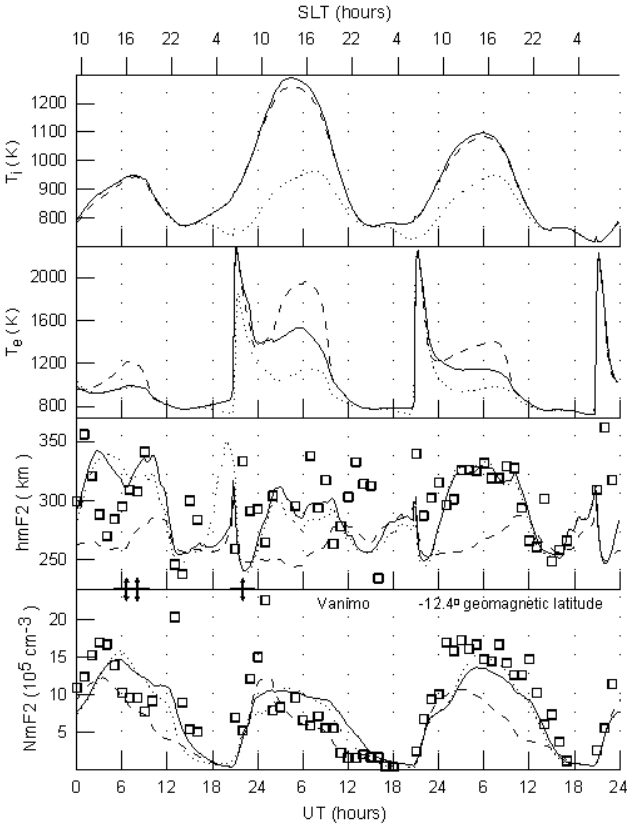

Fig. 5. From bottom to top, observed (squares) and calculated (lines) of $NmF2$, $hmF2$, electron temperatures and O^+ ion temperatures at the $F2$-region main peak altitude above the Vanimo ionosonde station during 25–27 August 1987. SLT is the solar local time at the Vanimo ionosonde station. The start times of the sudden commencement (06:58 UT on 25 August), main phase (08:00 UT on 25 August) and recovery phase (22:00 UT on 25 August) of the geomagnetic storm are indicated by the arrows. The curves are the same as in Fig. 4.

where the unit of UT is hour. As was pointed out before, we expect that the NRLMSISE-00 neutral model has some inadequacies in predicting the number densities with accuracy, and we have to change the number densities by correction factors at all altitudes to bring the modeled electron densities into agreement with the measurements. As a result of the comparison between the modeled $NmF2$ and $NmF2$ measured by the Manila ionosonde station (see Fig. 6), the value of [O] was increased by a factor of 2 in the 0–5° geomagnetic latitude range of the Northern Hemisphere at all altitudes from 02:00 UT to 08:00 UT on 26 August. During this time period, the [O] correction factor varies linearly from 2 to 1 in the geomagnetic latitude ranges between 5° and 15° and between 0° and −10°. To bring the measured and modeled electron densities into agreement above the Darwin and Vanimo ionosonde stations, the value of [O] was increased by a factor of 1.5 at the geomagnetic latitudes from −15° to −40° at all altitudes from 23:00 UT on 25 August to 02:00 UT on 26 August. To make the measured and modeled $NmF2$ agree over the Okinawa, Yamagawa, Kokubunji, and Akita ionosonde stations, the model [O] was decreased by a factor of 1.5 at the geomagnetic latitudes from 15° to 40° at all altitudes from 22:00 UT on 24 August to 09:00 UT on 25 August, while the model $[N_2]$ and $[O_2]$ were increased by a factor of 2 in the 15–40° geomagnetic latitude range

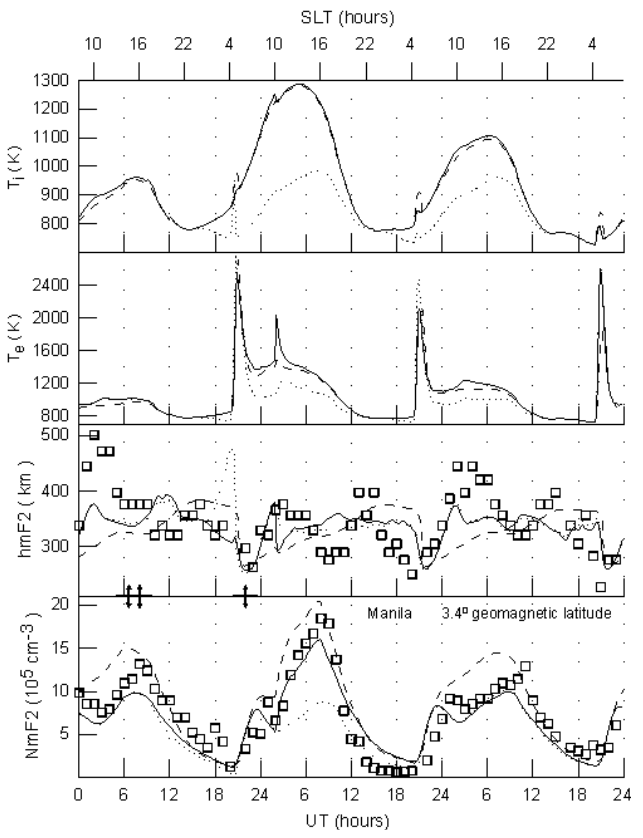

Fig. 6. From bottom to top, observed (squares) and calculated (lines) of $NmF2$, $hmF2$, electron temperatures and O^+ ion temperatures at the $F2$-region main peak altitude above the Manila ionosonde station during 25–27 August 1987. SLT is the solar local time at the Manila ionosonde station. The start times of the sudden commencement (06:58 UT on 25 August), main phase (08:00 UT on 25 August) and recovery phase (22:00 UT on 25 August) of the geomagnetic storm are indicated by the arrows. The curves are the same as in Fig. 4.

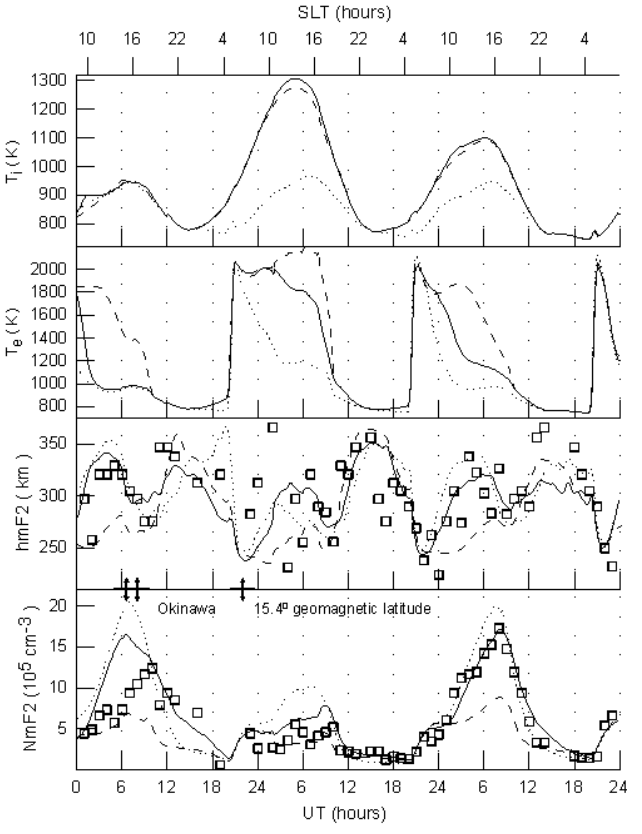

Fig. 7. From bottom to top, observed (squares) and calculated (lines) of $NmF2$, $hmF2$, electron temperatures and O^+ ion temperatures at the $F2$-region main peak altitude above the Okinawa ionosonde station during 25–27 August 1987. SLT is the solar local time at the Okinawa ionosonde station. The start times of the sudden commencement (06:58 UT on 25 August), main phase (08:00 UT on 25 August) and recovery phase (22:00 UT on 25 August) of the geomagnetic storm are indicated by the arrows. The curves are the same as in Fig. 4.

at all altitudes from 02:00 UT to 08:00 UT on 26 August. During these time periods, a linear variation in the [O] correction factor from 1.5 to 1 is assumed in the geomagnetic latitude range between $-15°$ and $-10°$ and between 15° and 10°, respectively, while a linear variation in the [N_2] and [O_2] correction factor from 2 to 1 is assumed in the geomagnetic latitude range between 15° and 5°.

Variations in $hmF2$ are predominantly determined by variations in the thermospheric wind at the ionosonde stations, such as Akita, Kokubunji, and Darwin and over the MU radar, which locations that are far enough from the geomagnetic equator (Rishbeth, 2000; Souza et al., 2000; Pincheira et al., 2002; Pavlov, 2003; Pavlov et al., 2004), i.e. effects of the $\boldsymbol{E}\times\boldsymbol{B}$ plasma drift on $hmF2$ and $NmF2$ over these sounders and over the MU radar are much less than those caused by the plasma drift due to the neutral wind. The HWW90 wind velocities are known to differ from observations (Titheridge, 1995; Kawamura et al., 2000; Emmert et al., 2001; Fejer et al., 2002). To bring the modeled and measured $hmF2$ and $NmF2$ into reasonable agreement over the Akita, Kokubunji, and Darwin sounders and over the MU radar, the meridional neutral wind, W, taken from the HWW90 wind model, is changed to W+ΔW. The values of ΔW, shown in the low panel of Fig. 11, are used in the Northern Hemisphere above the geomagnetic latitude of 24° (solid line) and in the Southern Hemisphere below the geomagnetic latitude of $-24°$ (dashed line), while ΔW=0 at the geomagnetic equator. A square interpolation of ΔW is employed between $-24°$ and 0° and between 24° and 0° geomagnetic latitude.

To give an example of changes in the meridional neutral wind due to ΔW, the diurnal variations of the modeled meridional uncorrected HWW90 (dotted lines) and corrected (solid lines) neutral winds during 25–27 August 1987 at 300 km are shown in the middle and top panels over the MU radar and over the Darwin ionosonde station, respectively. We conclude that the storm-time meridional wind velocity has non-regular variations, in agreement with the early

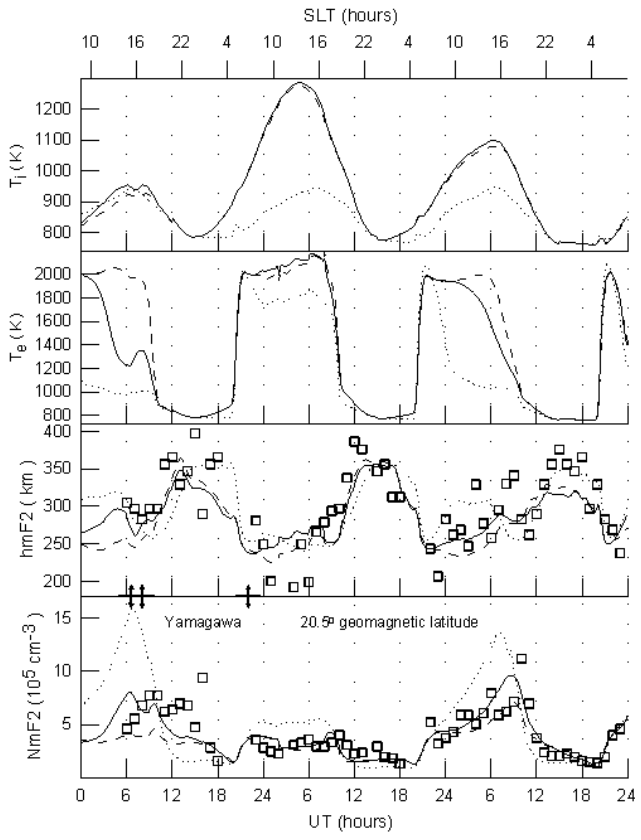

Fig. 8. From bottom to top, observed (squares) and calculated (lines) of $NmF2$, $hmF2$, electron temperatures and O^+ ion temperatures at the $F2$-region main peak altitude above the Yamagawa ionosonde station during 25–27 August 1987. SLT is the solar local time at the Yamagawa ionosonde station. The start times of the sudden commencement (06:58 UT on 25 August), main phase (08:00 UT on 25 August) and recovery phase (22:00 UT on 25 August) of the geomagnetic storm are indicated by the arrows. The curves are the same as in Fig. 4.

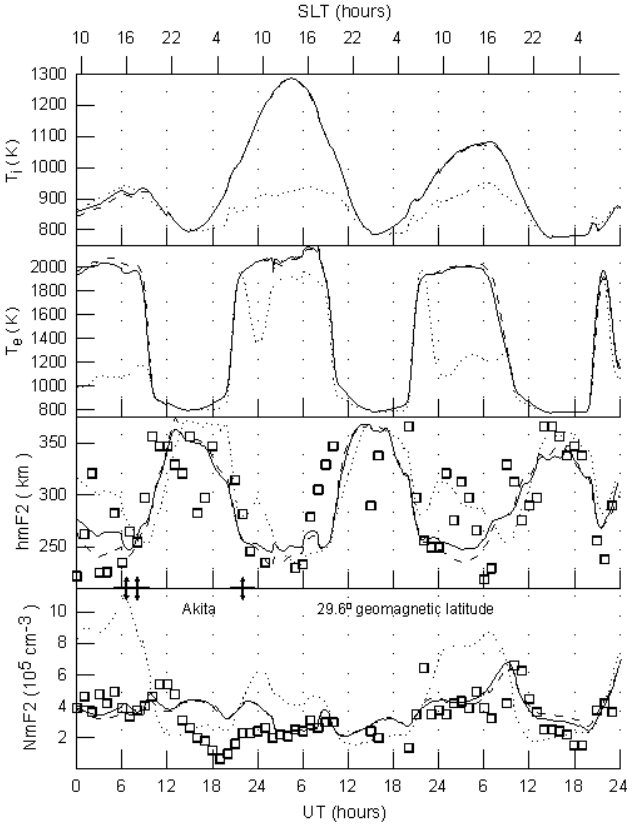

Fig. 9. From bottom to top, observed (squares) and calculated (lines) of $NmF2$, $hmF2$, electron temperatures and O^+ ion temperatures at the $F2$-region main peak altitude above the Akita ionosonde station during 19–21 March 1988. SLT is the solar local time at the Akita ionosonde station. The start times of the sudden commencement (06:58 UT on 25 August), main phase (08:00 UT on 25 August) and recovery phase (22:00 UT on 25 August) of the geomagnetic storm are indicated by the arrows. The curves are the same as in Fig. 4.

conclusions of Kawamura (2003), and the magnitude of the storm-time meridional wind shown by the solid line in the middle panel of Fig. 11 is comparable with that observed by the MU radar during disturbed conditions of 23 March–2 April 2001 studied by Kawamura (2003).

The solid lines in Figs. 4–10 show the results obtained from the model of the ionosphere and plasmasphere using the corrected NRLMSISE-00 neutral temperature and densities, the corrected meridional HWW90 wind, and the corrected zonal electric field. We conclude that the use of the corrected [O], [N_2], [O_2], T_n, W, and E_Λ brings the measured and modeled $NmF2$, $hmF2$, T_e, and T_i into reasonable agreement although there are some quantitative differences.

One can see from Fig. 6 that the NRLMSISE-00 model with the modified [O] improves the agreement with the measured $NmF2$ over the Manila ionosonde station. On the other hand, the NRLMSISE-00 model can have some inadequacies in predicting the actual [N_2] and [O_2] with accuracy. However, to reach approximately the same agreement between the measured and modeled $NmF2$ over the Manila ionosonde station, the values of the NRLMSISE-00 [N_2] and [O_2] must be decreased by a factor of 3–3.5 in the 0–5° geomagnetic latitude range of the Northern Hemisphere from 02:00 UT to 08:00 UT on 26 August at all altitudes without NRLMSISE-00 [O] corrections. If the NRLMSISE-00 [O] Southern Hemisphere correction, which is described above, is not used, then the values of the NRLMSISE-00 [N_2] and [O_2] must be decreased by a factor of 2 at the geomagnetic latitudes from $-15°$ to $-40°$ at all altitudes from 23:00 UT on 25 August to 02:00 UT on 26 August, to bring the measured and modeled $NmF2$ over the Darwin and Vanimo ionosonde stations into approximately the same agreement. Thus, the comparison between the NRLMSISE-00 [N_2] and [O_2] decrease, and the NRLMSISE-00 [O] increase does not show similarity and consistency in the magnitudes of their effects on $NmF2$ at low geomagnetic latitudes. This difference in the response of the calculated $NmF2$ to neutral density variations is large enough to provide evidence in favor of changing [O] in comparison with changing [N_2] and [O_2].

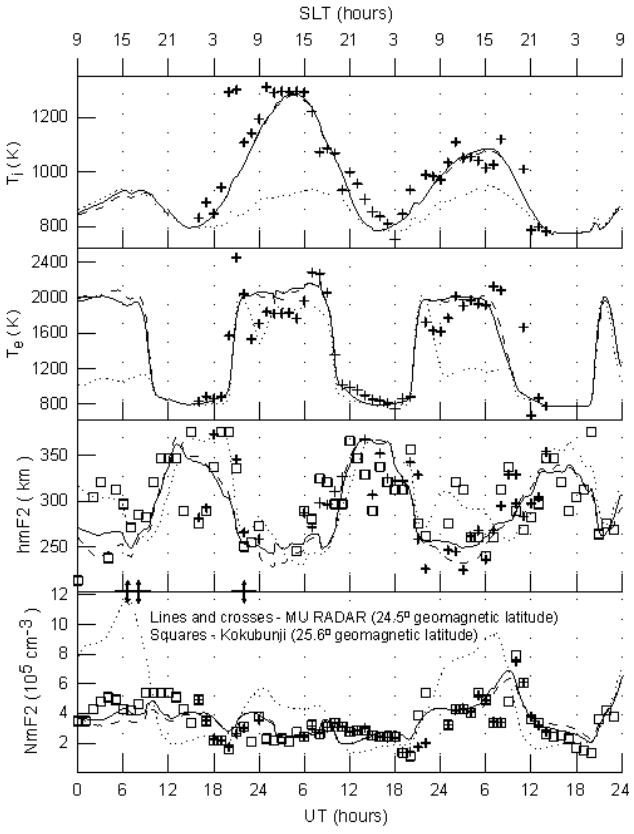

Fig. 10. Observed (crosses) and calculated (lines) $NmF2$ and $hmF2$ (two lower panels), and electron and O^+ ion temperatures (two upper panels) at the $F2$-region main peak altitude above the MU radar during 25–27 August 1987. SLT is the solar local time at the MU radar. Squares in the two lower panels show the measured $NmF2$ and $hmF2$ during 25–27 August 1987 above the Kokubunji ionosonde station. The start times of the sudden commencement (06:58 UT on 25 August), main phase (08:00 UT on 25 August) and recovery phase (22:00 UT on 25 August) of the geomagnetic storm are indicated by the arrows. The curves are the same as in Fig. 4 (see first paragraph of Sect. 4.2).

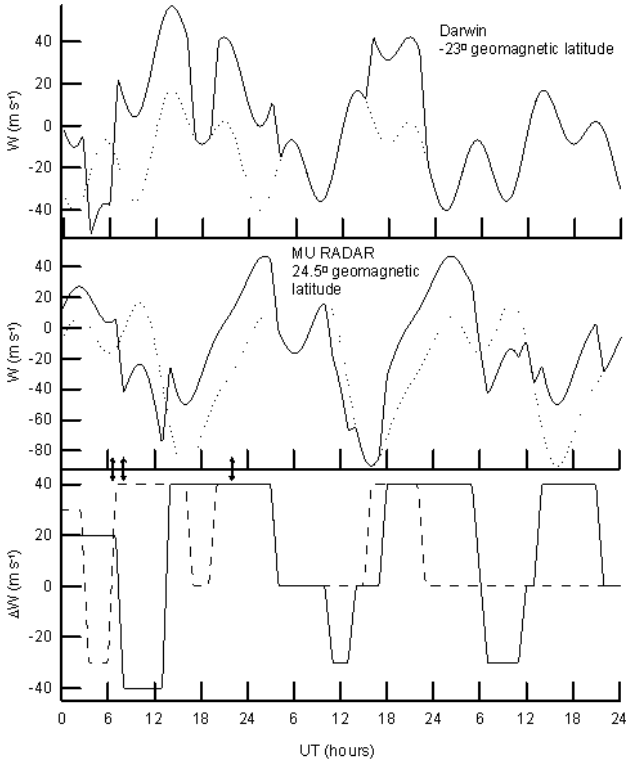

Fig. 11. Diurnal variations of the meridional HWW90 neutral wind, W, the correction, ΔW, of W during 25–27 August 1987 (when the original value of W is changed to W+ΔW). The values of ΔW shown in the low panel are used in the Northern Hemisphere above the geomagnetic latitude of 24° (solid line) and in the Southern Hemisphere below the geomagnetic latitude of $-24°$ (dashed line), while ΔW=0 at the geomagnetic equator. A square interpolation of ΔW is employed between $-24°$ and 0° and between 24° and 0°. The modeled meridional uncorrected HWW90 (dotted lines) and corrected (solid lines) neutral winds at 300 km are shown in the middle and top panels over the MU radar and over the Darwin ionosonde station, respectively. The meridional HWW90 wind is directed northward for W>0 and southward for W<0. The start times of the sudden commencement (06:58 UT on 25 August), main phase (08:00 UT on 25 August) and recovery phase (22:00 UT on 25 August) of the geomagnetic storm are indicated by the arrows.

It is well known that $NmF2$ is proportional to [O]/[N_2] in the middle-latitude daytime ionosphere (e.g. Rishbeth and Garriot, 1969; Rees, 1989; Lobzin and Pavlov, 2002, and references therein). However, the low-latitude ionosphere is special because of the constraints imposed on electron and ion motions by the magnetic field and by the zonal electric field. In agreement with the results of Pavlov et al. (2004), the model calculations of this work provide an additional evidence that the dependence of $NmF2$ on [N_2] and [O_2] is weaker than the dependence of $NmF2$ on [O] by day at low geomagnetic latitudes, i.e. $NmF2$ is not proportional to [O]/[N_2] or to [O]/[O_2] in the low-latitude daytime ionosphere.

To evaluate the relative role of the $\boldsymbol{E}\times\boldsymbol{B}$ drift and possible uncertainties in E_Λ in variations of N_e, N_i, T_e, and T_i, calculations have been carried out from the model when the value of E_Λ, used in producing results shown by solid lines, was divided by a factor of 10 at all the studied geomagnetic latitudes and when the corrections of the NRLMSISE-00 temperature and densities and meridional neutral HWW90 wind are the same as for the solid lines in Figs. 4–10. The model results are shown by dashed lines in Figs. 4–10.

During most of the daytime period, the $\boldsymbol{E}\times\boldsymbol{B}$ drift lifts the plasma from lower field lines to higher field lines, while during most of the nighttime period, this drift moves ions and electrons from higher to lower magnetic field lines. Simultaneously, the plasma diffuses along the magnetic field lines. The comparison between the solid and dashed lines in the bottom panel of Fig. 6 shows that, close to the geomagnetic equator, the $NmF2$ enhancement caused by the decrease in the plasma outflow is stronger than the reduction in $NmF2$ caused by the increase in the loss rate of $O^+(^4S)$ ions.

Therefore, the weakening of E_Λ leads to the $NmF2$ increase by day over the Manila sounder. The nighttime $NmF2$ increase is a result of the daytime $NmF2$ increase and the decrease in the loss rate of $O^+(^4S)$ ions due to the $hmF2$ increase caused by the weakening of E_Λ.

The complex interplay of the physical processes described above for the Manila sounder determines the variations in $NmF2$ and $hmF2$ caused by the weakening of E_Λ over the other sounders. Figures 4–10 show that the magnitude of the change in $NmF2$ caused by the weakening of E_Λ by a factor of 10 is decreased if the absolute value of the geomagnetic latitude is increased. As an example, above the Akita ionosonde station, this weakening in E_Λ changes $NmF2$ and $hmF2$ up to a factor of 0.85–1.21 and up to the maximum value of 25 km, respectively, while the maximum electron density change is a factor of 0.83–1.5 at 400 km. In agreement with the previous study by Pavlov et al. (2004), we conclude that the use of the one-dimensional time dependent model of the ionosphere and plasmasphere, which does not take into account the $\boldsymbol{E}\times\boldsymbol{B}$ plasma drift, leads to noticeable errors in the calculated daytime electron density of the $F2$ region and a part of the topside ionosphere, even at geomagnetic latitudes of about $25°-30°$.

The measured $hmF2$ presented in Figs. 4–10 show large fluctuations. The possible source of this scatter in $hmF2$ is the dependence of $hmF2$ on $M(3000)F2$ and ΔM given by Dudeney (1983) (see Sect. 3), which determines $hmF2$ diurnal variations with errors. Furthermore, there are no foE measurements over Manila during 25-27 August, i.e. it is suggested that ΔM=0. It means that the measured $hmF2$ presented in Fig. 6 can be overestimated (Dudeney, 1983). The ionosondes listed in Table 1 are not located at the geomagnetic longitudes of 201°, which is used in the model calculations. This geomagnetic longitude displacement can explain a part of the disagreement between the modeled and measured $hmF2$, $NmF2$, T_e, and T_i in Figs. 4–10. A part of these discrepancies is probably due to the uncertainties in the model inputs, such as a possible inability of the NRLMSIS-00 model to accurately predict the densities and temperature for the studied period at low-latitudes, and uncertainties in the neutral wind, EUV fluxes, chemical rate coefficients, photoionization, photoabsorption and electron impact cross sections for N_2, O_2, and O.

4.3 Latitude variations in $NmF2$ and $hmF2$

The comparison between the measured (crosses) and modeled (lines) $NmF2$ and $hmF2$ latitude variations is depicted in Figs. 12, 14, and 16 at 02:00 UT (two lower panels) and 05:00 UT (two upper panels) and in Figs. 13, 15, and 17 at 08:00 UT (two lower panels) and 11:00 UT (two upper panels) on 25 August (Figs. 12 and 13), 26 August (Figs. 14 and 15), and 27 August (Figs. 16 and 17). The combinations of the model input parameters used in the calculations of the model results, shown by the solid lines, are the same as those for the solid lines in Fig. 4. The dashed lines show the results produced by the model using the combinations of $E_\Lambda^{\rm eff}$ based on the zonal electric field given by the dashed lines in Fig. 1 (i.e. the zonal electric field for geomagnetically quiet conditions taken from Fejer (1993) and Scherliess and Fejer (1999) is used), the HWW90 wind velocities, the NRLMSISE-00 neutral densities and temperature with the same corrections of W, [O], $[N_2]$, $O_2]$, and T_n as for the solid lines. The dotted lines show the results produced by the model using the combinations of $E_\Lambda^{\rm eff}$ based on the corrected zonal electric field given by crosses in Fig. 1, zero neutral wind, and the NRLMSISE-00 neutral densities and temperature with the same corrections of the NRLMSISE-00 neutral densities and temperature as for the solid lines.

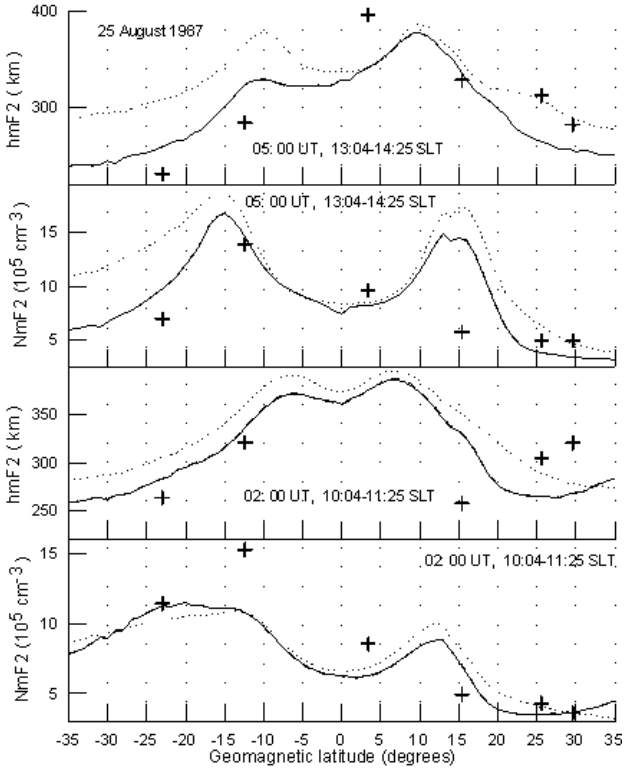

Fig. 12. Observed (crosses) and calculated (lines) $hmF2$ and $NmF2$ at 02:00 UT (two lower panels) and 05:00 UT (two upper panels) on 25 August 1987. The measured $hmF2$ and $NmF2$ are taken from the ionospheric sounder station listed in Table 1. The solid curves are the same as in Fig. 4. The dotted lines show the results produced by the model, using the combinations of $E_\Lambda^{\rm eff}$ based on the corrected zonal electric field, given by crosses in Fig. 1 (as for the solid lines in Fig. 12), zero neutral wind, and the NRLMSISE-00 neutral densities and temperature with the same corrections of [O] and T_n as for the solid lines in Fig. 12. The dashed lines show the results produced by the model, using the combinations of $E_\Lambda^{\rm eff}$ based on the zonal electric field, given by the dashed lines in Fig. 1, and the HWW90 wind velocities, the NRLMSISE-00 neutral densities and temperature with the same corrections of W, [O], $[N_2]$, $[O_2]$, and T_n as for the solid lines in Fig. 12.

By comparing the results of calculations presented by the solid lines in Figs. 12, 13, 16, and 17, the similarity of the equatorial anomaly on 25 and 27 August can be seen. If

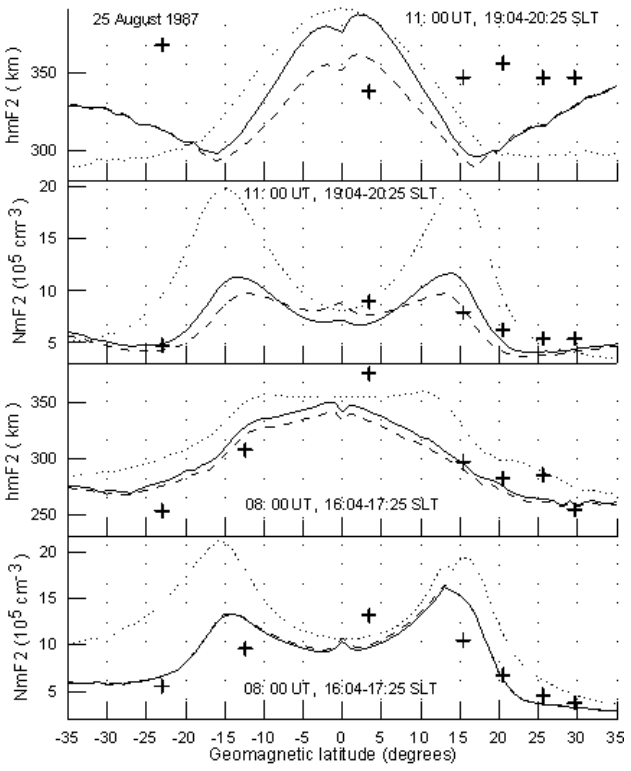

Fig. 13. Observed (crosses) and calculated (lines) $hmF2$ and $NmF2$ at 08:00 UT (two lower panels) and 11:00 UT (two upper panels) on 25 August 1987. The measured $hmF2$ and $NmF2$ are taken from the ionospheric sounder station listed in Table 1. The curves are the same as in Fig. 12.

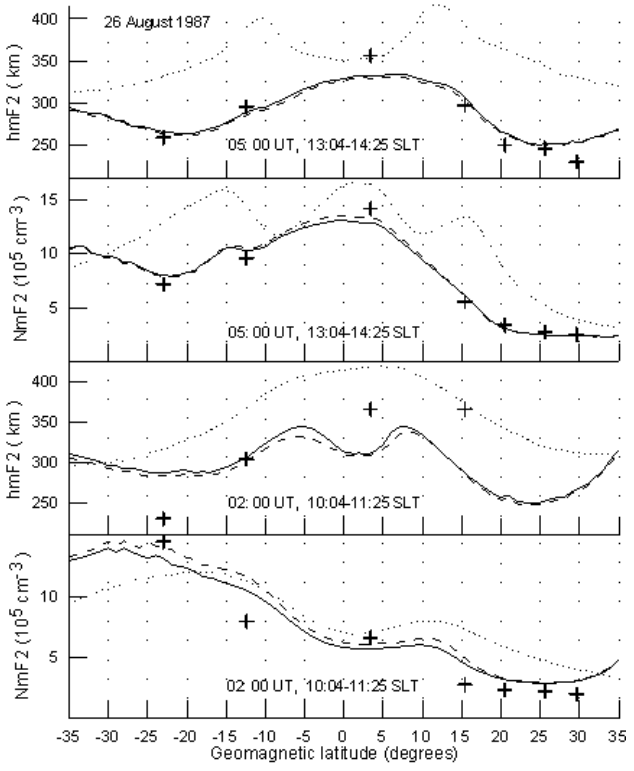

Fig. 14. Observed (crosses) and calculated (lines) $hmF2$ and $NmF2$ at 02:00 UT (two lower panels) and 05:00 UT (two upper panels) on 26 August 1987. The measured $hmF2$ and $NmF2$ are taken from the ionospheric sounder station listed in Table 1. The curves are the same as in Fig. 12.

we compare these solid lines with those in Figs. 14 and 15, we can conclude that the geomagnetic latitude variations in the electron density calculated for 26 August 1987 (the recovery phase of the geomagnetic storm) differ significantly from those calculated for 25 August 1987 (the initial and main phases of the geomagnetic storm and before SSC) and for 27 August 1987 (after the geomagnetic storm). The model calculations presented in Figs. 12, 13, 16, and 17 shows that the equatorial plasma fountain, responsible for the equatorial anomaly formation, undergoes significant inhibition on 26 August. During 25 and 27 August, the model produces the onset of the equatorial anomaly crest formation near 01:00–01:30 UT and the crests disappear close to 14:00 UT, while a geomagnetic latitude electron density profile with two equatorial anomaly crests is distinguished from 01:00 UT to 04:00 UT on 26 August. The principal feature of the equatorial anomaly is the crest-to-trough ratio. The modeled $NmF2$ show that the equatorial anomaly effect is most pronounced close to 06:00 UT on 25 and 27 August.

It follows from the model results, shown by the solid lines of Figs. 12, 13, 16, and 17, that the latitude variations of the $hmF2$ and $NmF2$ are asymmetrical about the geomagnetic equator on 25 and 27 August. As seen from a comparison between the solid lines of Figs. 14 and 15 and those of Figs. 12, 13, 16, and 17, the north-south asymmetry in $NmF2$ is much stronger on 26 August than that on 25 or 27 August. Figure 12 shows that the features of the $NmF2$ and $hmF2$ daytime latitude variations from 02:00 UT to 05:00 UT on 25 August before SSC are a greater anomaly crest value of $NmF2$ in the winter hemisphere and a greater maximum value of $hmF2$ in the summer hemisphere. It is seen from the comparison between the corresponding solid lines in Figs. 12 and 14 that there are none of these features in the $NmF2$ and $hmF2$ from 02:00 UT to 05:00 UT on 26 August at the recovery phase of the geomagnetic storm.

It is clear that the north-south asymmetry in $NmF2$ and $hmF2$ should come about through the asymmetry in neutral temperature, densities, and winds relative to the geomagnetic equator. The calculations show that the thermospheric circulation produced by the HWW90 model is not symmetric relative to the geomagnetic equator during 25–27 August 1987 (e.g. the middle and top panels of Fig. 11). As can be seen from the comparison between the corresponding solid and dotted lines in Figs. 12–13 and 16–17, the asymmetry in $hmF2$ and $NmF2$ is decreased if the model uses zero neutral wind. We conclude that the asymmetry in the neutral wind given by the HWW90 model determines most of the asymmetry in $hmF2$ and $NmF2$ between the northern and southern geomagnetic hemispheres on 25 and 27 August from about 01:00–01:30 UT to about 14:00 UT when

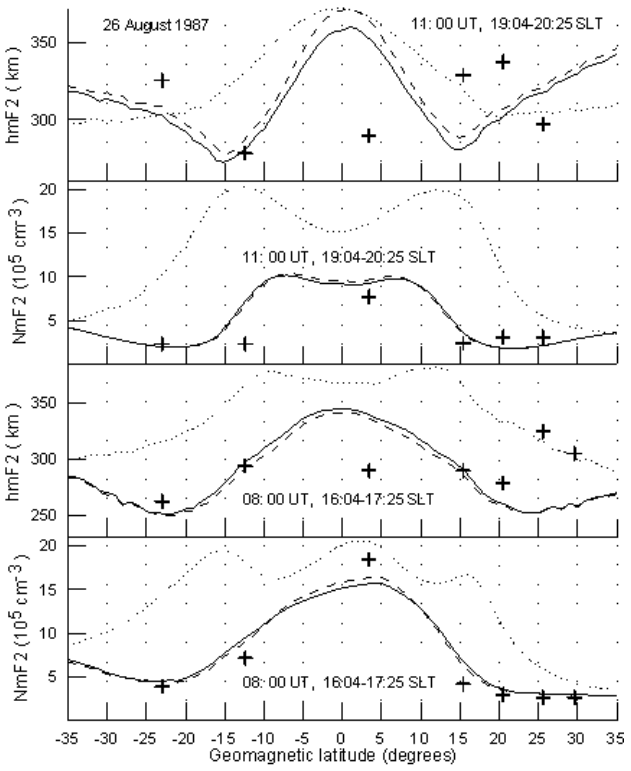

Fig. 15. Observed (crosses) and calculated (lines) $hmF2$ and $NmF2$ at 08:00 UT (two lower panels) and 11:00 UT (two upper panels) on 26 August 1987. The measured $hmF2$ and $NmF2$ are taken from the ionospheric sounder station listed in Table 1. The curves are the same as in Fig. 12.

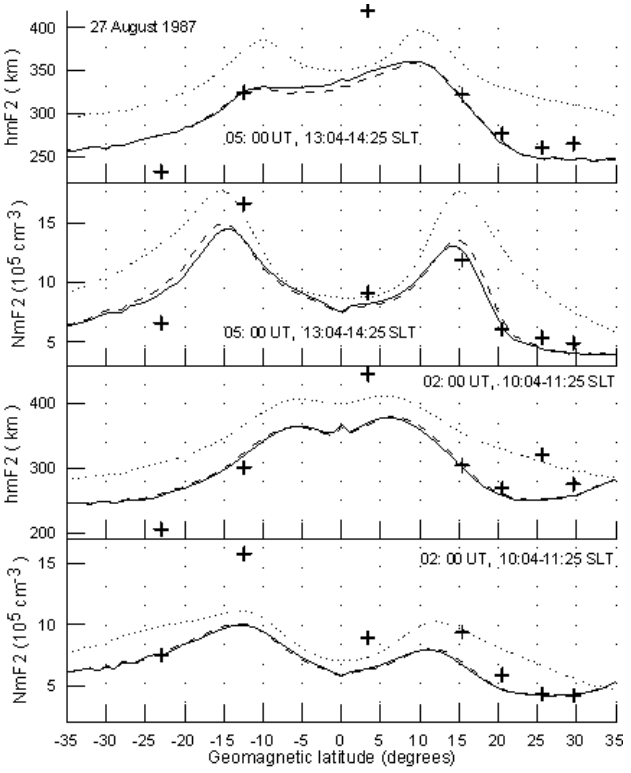

Fig. 16. Observed (crosses) and calculated (lines) $hmF2$ and $NmF2$ at 02:00 UT (two lower panels) and 05:00 UT (two upper panels) on 27 August 1987. The measured $hmF2$ and $NmF2$ are taken from the ionospheric sounder station listed in Table 1. The curves are the same as in Fig. 12.

the equatorial anomaly exists in the ionosphere. By comparing the corresponding solid and dotted lines in Figs. 14 and 15, it is seen that both asymmetries in neutral winds and in neutral temperature and densities relative to the geomagnetic equator are responsible for the north-south asymmetry in $NmF2$ and $hmF2$ on 26 August.

The differences between the disturbed (crosses in the bottom and middle panels of Fig. 1) and quiet (dashed lines in the bottom and middle panels of Fig. 1) zonal electric fields, which are most pronounced from 14:00–16:00 UT to 20:00–23:00 UT, cause the corresponding noticeable variations in the calculated $NmF2$ from about 16:00–17:00 UT to about 20:00–22:00 UT. Taking, for example, the Manila sounder, we found that the effects of disturbances in the zonal electric field lead to the increase in $NmF2$ by a factor of 1.2–2.5 from 16:14 UT to 21:04 UT on 25 August, by a factor of 1.2–3.0 from 17:04 UT to 21:14 UT on 26 August, and by a factor of 1.2–2.5 from 17:54 UT to 20:50 UT on 27 August. On the other hand, the comparison between the corresponding solid and dashed lines in Figs. 12–17 show that the effects of disturbances in the zonal electric field on $NmF2$ and $hmF2$ is hardly distinguished from 02:00 UT to 05:00 UT on 25 August, from 05:00 UT to 08:00 UT on 26 August, and from 02:00 UT to 11:00 UT on 27 August. We conclude from the model calculations that the storm-time changes in the zonal electric field are not responsible for the suppression of the equatorial anomaly on 26 August, due to weak differences between the disturbed and quiet zonal electric fields on 26 August.

It can be seen from the comparison of the corresponding solid and dotted lines in Figs. 12–17 that the relative contributions of the meridional wind in $hmF2$ and $NmF2$ latitude variations vary with time. We found that close to the geomagnetic equator displacements of $hmF2$ and variations in $NmF2$, caused by the effects of neutral winds on $hmF2$ and $NmF2$, are stronger on 26 August than those on 25 and 27 August from 02:00 UT to 11:00 UT. It is interesting to point out that the neutral winds inhibit the development of the equatorial anomaly, leading to a decrease in the crest-to-trough ratio during 25–27 August 1987 (compare the corresponding solid and dotted lines in Figs. 12–17).

On the other hand, the model using the combinations of the corrected HWW90 wind velocities, the corrected storm-time zonal electric field, and the original NRLMSISE-00 neutral densities and temperature produces the equatorial anomaly from about 01:00 UT to about 09:00 UT on 26 August. We conclude that the storm-time changes in the neutral densities (due to the correction in the NRLMSISE-00 neutral densities on 26 August described in Sect. 4.2) are also responsible for the equatorial anomaly inhibition on 26 August.

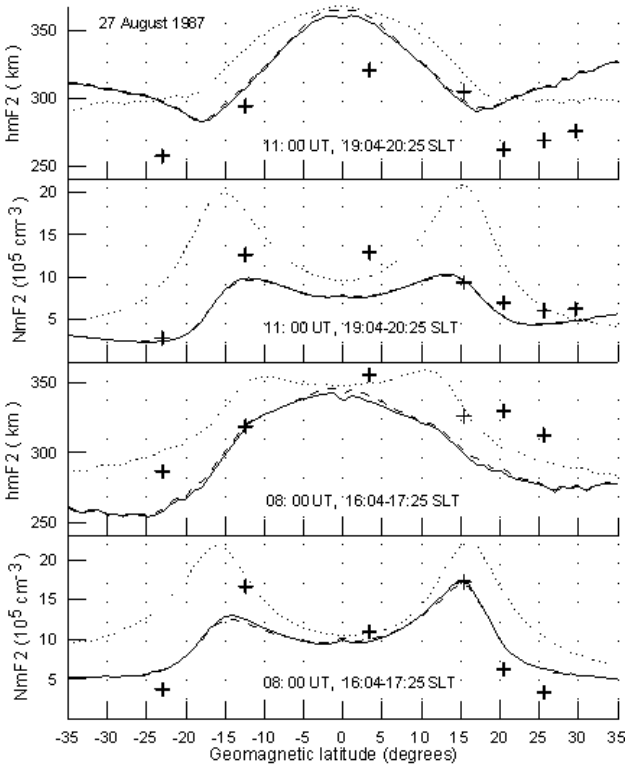

Fig. 17. Observed (crosses) and calculated (lines) $hmF2$ and $NmF2$ at 08:00 UT (two lower panels) and 11:00 UT (two upper panels) on 27 August 1987. The measured $hmF2$ and $NmF2$ are taken from the ionospheric sounder station listed in Table 1. The curves are the same as in Fig. 12.

The equatorial $hmF2$ and $NmF2$ are not expected to be very sensitive to neutral wind variations, since these variations cannot induce significant vertical motions at the geomagnetic equator. However, variations in the neutral wind affect electron and ion densities at nonzero geomagnetic latitudes, causing corresponding variations in electron and ion densities at all points of these magnetic field lines through diffusion of ions and electrons along the magnetic field lines. The $\boldsymbol{E}\times\boldsymbol{B}$ drift of electrons and ions redistribute these changes in electron and ion densities between field lines. As a result, variations in the neutral wind at nonzero geomagnetic latitudes can lead to changes in electron density altitude profiles close to the geomagnetic equator, resulting in corresponding variations of equatorial $hmF2$ and $NmF2$. It is necessary to point out that N_e changes more slowly with altitude close to geomagnetic equator at F-region altitudes and in the topside ionosphere in comparison with altitude changes in N_e at middle geomagnetic latitudes. Therefore, small variations in N_e near $hmF2$ can change $hmF2$ close to the geomagnetic equator. The neutral wind causes large north-south asymmetries in N_e. As a result, the use of zero neutral wind instead of the corrected HWW90 wind causes strong electron density changes in the Northern and Southern Hemispheres, resulting in $NmF2$ and $hmF2$ changes shown in Figs. 12–17. This change in W is more pronounced on 26 August in comparison with that on 25 and 27 August (see, for example, the magnitudes of W shown by the solid lines in the middle and top panels of Fig. 11). As a result, displacements of $hmF2$ and variations in $NmF2$, caused by the effects of neutral winds on $hmF2$ and $NmF2$, are stronger on 26 August than those on 25 and 27 August.

It is found by Pavlov (2003) and Pavlov et al. (2004) that the daytime magnitude of $NmF2$ is reduced up to a maximum factor of 1.44 and 1.16 between $-30°$ and $+30°$ of the geomagnetic latitude, due to enhanced vibrational excitation of N_2 and O_2 during quiet conditions at high and moderate solar activities, respectively. We found that, in the plane of the geomagnetic meridian at the geomagnetic longitude of 201°, the increase in the loss rate of $O^+(^4S)$ ions, due to the vibrational excited N_2 and O_2, causes the maximum decrease in the calculated $NmF2$ by a factor of 1.12, 1.26, and 1.13 and the maximum change in the calculated $hmF2$ of 4, 11, and 4 km in the low-latitude ionosphere between $-30°$ and $+30°$ of the geomagnetic latitude at low solar activity on 25, 26, and 27 August, respectively. It is interesting to point out that, in this latitude range, the maximum decrease in the calculated electron density, caused by reactions of $O^+(^4S)$ ions with vibrationally excited N_2 and O_2, is a factor of 1.10 (1.07), 1.35 (1.22), and 1.15 (1.09) at 250 (300) km altitude on 25, 26, and 27 August, respectively. The average daytime neutral temperature is greater on 26 August than that on 25 August or 27 August, due to the correction factor given by Eq. (4). Figures 4–10 show that the average daytime electron temperature is less on 25 August or 27 August than that on 26 August. As a result, the vibrational temperatures of N_2 and O_2 are largest on 26 August, and the resulting effect of vibrationally excited N_2 and O_2 on the electron density of the low-latitude ionosphere is largest on 26 August. It is possible to point out that the increase in the $O^+(^4S)$ loss rate due to vibrationally excited O_2 is less than that due to vibrationally excited N_2. The difference between the N_2 vibrational temperature and the neutral temperature is less than 167 K, 364 K, and 270 K, and this difference is larger than -184 K, -202 K, and -15 K at $hmF2$ between $-30°$ and $+30°$ of the geomagnetic latitude on 25, 26, and 27 August, respectively.

4.4 Electron and ion temperature variations

The two upper panels of Figs. 4–10 show the calculated (lines) electron, T_e, and ion, T_i, temperatures at the $F2$-region main peak altitude for the 25–27 August 1987 time period above the Darwin (Fig. 4), Vanimo (Fig. 5), Manila (Fig. 6), Okinawa (Fig. 7), Yamagawa (Fig. 8), and Akita (Fig. 9) ionosonde stations and above the MU radar (Fig. 10). Crosses in the two top panels of Fig. 10 show the electron and ion temperatures measured by the MU radar at $hmF2$ during 25–27 August 1987. If we take into account the accuracy of the MU radar electron and ion temperature measurements (Sato et al., 1989) and uncertainties of model calculations, then we conclude that the electron and ion temperatures observed by the MU radar are in reasonable agreement with the model results, shown by the solid lines in the two upper

panels of Fig. 10, although there are some quantitative differences. The reasonable agreement between the measured radar electron and ion temperature, and the modeled electron and ion temperature, determines the reliability of the calculated T_e and T_i at other geomagnetic latitudes.

It is evident from the comparison between the corresponding solid and dashed lines in the two top panels of Figs. 4–10 that the correction in the disturbed $\boldsymbol{E}\times\boldsymbol{B}$ drift produces negligible effects in T_i during 25–27 August 1987, while there are some electron temperature variations due to this input model parameter change. By comparing the results of the model calculations presented by the corresponding solid and dotted lines in Figs. 4–10, it can be seen that the electron temperature is affected by the corrections in the model HWW90 wind, and in the NRLMSISE-00 neutral temperature and densities.

It follows from the model calculations (see solid lines in Figs. 4–10) that the diurnal solar local time variations of T_e are characterized by morning peaks above the Darwin Vanimo, Manila, and Okinawa ionosonde stations during 26–28 August, and above the Akita ionosonde station and the MU radar on 28 August, and by feebly marked morning electron temperature peaks over the Yamagawa ionosonde station on 27 and 28 August. The model produces evening peaks in the diurnal solar local time electron temperature variations over the MU radar (on 25 August), the Darwin (on 25–27 August), Vanimo (on 26 August), Yamagawa (on 25 and 26 August), and Akita (on 25 and 26 August) ionosonde stations. A broad evening-daytime maximum in the electron temperature is calculated above Manila and Okinawa on 25 August and over Vanimo on 25 and 27 August.

The electron-ion cooling rate of thermal electrons, which is the predominant cooling rate at $hmF2$ and the main cooling rate in the plasmasphere and topside ionosphere, is proportional to N_e squared. As a result, variations in N_e cause variations in T_e.

It follows from the electron and ion temperatures profiles measured at Jicamarca that the enlargement of the altitude region with $T_e > T_i$ occurs at sunrise at all heights to at least 600 km (McClure, 1969). The model calculations show that at sunrise, there is a rapid heating of the ambient electrons by photoelectrons, and the difference between the electron and neutral temperatures could be increased because nighttime electron densities are less than those by day, and the electron cooling during morning conditions is less than that by day. This expands the altitude region at which $T_e > T_i$ near the equator and can lead to the sunrise electron temperature peaks at $hmF2$ altitudes. After the abrupt increase at sunrise, the electron temperature decreases, owing to the increasing electron density due to the increase in the cooling rate of thermal electrons. An appearance, a magnitude, and a disappearance of a morning electron temperature peak at $hmF2$ depend on a minimum value of the nighttime $NmF2$ before sunrise, because the morning $NmF2$ is a function of this minimum nighttime $NmF2$.

Like the middle-latitude F-region ionosphere, the nocturnal lowlatitude F-region is maintained due to the lowlatitude daytime F-region decay and by a downward flow of ionization from the plasmasphere. There is also a plasma inflow due to the ionospheric and plasmaspheric electrons and ions which are moved from middle to low geomagnetic latitudes by the downward nighttime $\boldsymbol{E}\times\boldsymbol{B}$ drift. It should be noted that the role of a downward flow of ionization from the plasmasphere is increased before sunrise. A plasma tube length and total plasma tube content are decreased with the lowering of the geomagnetic latitude. It means that an increase in the absolute value of the geomagnetic latitude can lead to an increase in a downward flow of ionization from the plasmasphere, the increase in the nighttime electron density before sunrise and the resulting decrease in the magnitude of the morning electron temperature peak.

The downward nighttime and morning $\boldsymbol{E}\times\boldsymbol{B}$ drift, resulting from $E_\Lambda < 0$, moves the ionospheric and plasmaspheric electrons and ions from middle to low geomagnetic latitudes, and ions and electrons then diffuse downward along the magnetic field lines (crosses in the bottom panel of Fig. 1 show that the value of E_Λ, when less or very close to zero, is correct over the geomagnetic equator from about 11:45 UT to about 22:45 UT on 25 August, from about 10:15 UT to about 22:25 UT on 26 August, and from about 10:30 UT to about 22:15 UT on 27 August). The resulting effect of these physical processes on $NmF2$ depends on the competition between an electron density enhancement caused by a plasma inflow and an electron density depletion due to an increase in the loss rate of $O^+(^4S)$ ions, owing to a $NmF2$ peak layer lowering.

It is interesting to illustrate the causes of the morning electron temperature peaks which exist in the electron temperature variations on 28 August over the MU radar and above all the ionosonde stations listed in Table 1 (see Figs. 4–10). Figure 18 shows the latitude dependence of the minimum nighttime $F2$ layer peak electron density (panel (a)), $NmF2_{\min}$, and its $F2$ peak altitude (panel (b)), $hmF2_{\min}$, the morning electron temperature peak (panel (d)), T_e^{peak}, and $NmF2_{\text{peak}}$ (panel (c)), which is the value of $NmF2$ for the point of the morning electron temperature peak calculation. The results, shown by the solid lines in Fig. 18, were calculated by the model with the corrected zonal electric field given by crosses in Fig. 1, the corrected HWW90 wind, and the corrected NRLMSISE-00 neutral temperature and densities. The dotted lines in Fig. 18 show the results produced by the model with the corrected zonal electric field given by crosses in Fig. 1, zero neutral wind for the time period after 12:00 UT on 27 August, and the NRLMSISE-00 neutral temperature and densities with the same correction as for the solid lines. The dashed lines in Fig. 18 show the results given by the model with the same corrections of the NRLMSISE-00 and HWW90 models as for the solid lines, and when the value of the corrected zonal electric field, used in producing results shown by solid lines, was divided by a factor of 10 at all the studied geomagnetic latitudes only for the time period after 12:00 UT on 27 August.

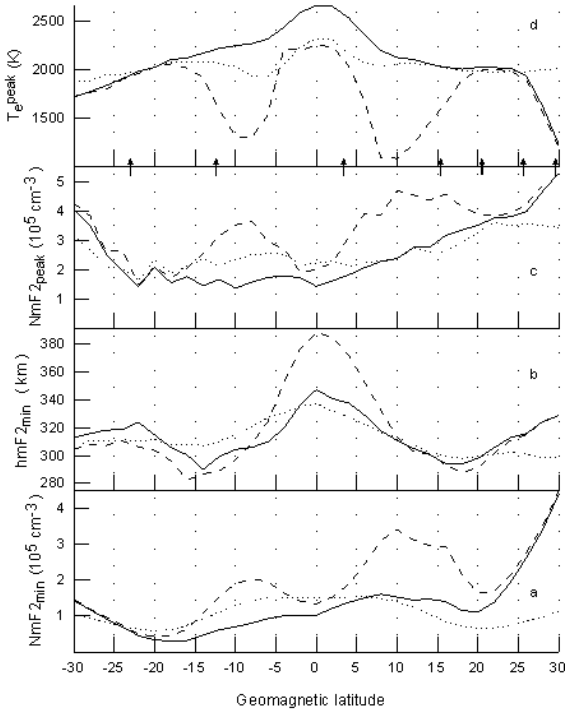

Fig. 18. The calculated minimum nighttime $F2$ layer peak electron density (panel (a)), $NmF2_{\min}$, and its $F2$ peak altitude, $hmF2_{\min}$ (panel (b)). The dependences of the calculated morning electron temperature peak, T_e^{peak}, on the geomagnetic latitude are presented in (panel (d)). The (panel (c)) shows the calculated $NmF2_{peak}$, which is $NmF2$ at the point of the morning electron temperature peak calculation. The solid lines show the results given by the model with the corrected equatorial zonal electric field, given by crosses in the bottom and middle panels of Fig. 1, the corrected HWW90 wind, and the corrected NRLMSISE-00 neutral temperature and densities. The dotted lines show the results produced by the model with the same value of the zonal electric field as for the solid lines, zero neutral wind only for the time period after 12:00 UT on 27 August 1987, and the NRLMSISE-00 neutral temperature and densities with the same corrections as for the solid lines. The results shown by dashed lines were calculated by the model with the same corrections of the NRLMSISE-00 neutral temperature and densities and meridional neutral HWW90 wind as for the solid lines, and when the value of the corrected zonal electric field, used in producing results, shown by solid lines, was divided by a factor of 10 at all the studied geomagnetic latitudes only for the time period after 12:00 UT on 27 August 1987. The solid, dotted and dashed lines in the panels (a,b) correspond to 04:40–05:12 SLT on 28 August (19:44–21:44 UT on 27 August), 04:30-05:18 SLT on 28 August (19:34–20:34 UT on 27 August), and 04:39–05:26 SLT on 28 August (19:43–20:44 UT on 27 August), respectively. The solid, dotted and dashed lines in the panels (c,d) correspond to 05:43–07:01 SLT on 28 August (20:54–22:24 UT on 27 August), 05:42–06:31 SLT on 28 August (20:54–21:54 UT on 27 August), and 06:03–07:11 SLT on 28 August (21:04–22:34 UT on 27 August), respectively. Arrows at the top mark the locations of the Darwin, Vanimo, Manila, Okinawa, Yamagawa, Kokubunji, and Akita sounders at $-23.0°$, $-12.4°$, $3.4°$, $15.4°$, $29.6°$, $20.5°$, $25.6°$, and $29.6°$ geomagnetic latitudes, respectively.

By comparing the solid lines in the panels (a,c) of Fig. 18, it is seen that the geomagnetic latitude variations of the $NmF2$ peak, whose value affects a morning electron temperature peak at $hmF2$ through changes in electron cooling rates, is similar to the dependence of $NmF2_{\min}$ on the geomagnetic latitude. As a result, the model calculations of this work provide evidence that an appearance, a magnitude, and a disappearance of a morning electron temperature peak at $hmF2$ depend on physical processes, which determine $NmF2_{\min}$.

It follows from the comparison between the corresponding solid and dashed lines in the panels (a,c) of Fig. 18 that the decrease in the equatorial nighttime downward $\boldsymbol{E}\times\boldsymbol{B}$ drift by a factor of 10 after 12:00 UT on 27 August leads to the increase in $NmF2$, i.e. the $NmF2$ reduction caused by the increase in the loss rate of $O^+(^4S)$ ions is stronger than the enhancement in $NmF2$ caused by the plasma inflow. The dashed line in the panel (a) of Fig. 18 shows that the equatorial anomaly caused by the upward $\boldsymbol{E}\times\boldsymbol{B}$ drift by day is maintained in the nighttime low-latitude ionosphere due to the low-latitude daytime F-region decay, and a downward flow of ionization from the plasmasphere is not important. As a result, we conclude that the nighttime and morning downward $\boldsymbol{E}\times\boldsymbol{B}$ drift causes the decrease in $NmF2$ and the resulting increase in the morning peak in T_e. The nighttime and morning downward $\boldsymbol{E}\times\boldsymbol{B}$ drift becomes more effective in lowering the electron density with the lowering of the geomagnetic latitude, i.e. a decrease in the absolute value of the geomagnetic latitude leads to a decrease in the electron density close to sunrise, resulting in an increase in the magnitude of the morning T_e peak. It follows from the panel (d) of Fig. 18 that the role of the nighttime and morning downward $\boldsymbol{E}\times\boldsymbol{B}$ drift in creating the morning electron temperature peak is negligible above about 20° and below about $-20°$ geomagnetic latitude.

To obtain a better understanding of the relative role of the plasma drift caused by the neutral wind in the formation of the morning electron temperature peak, the calculations have been carried out from the model when the values of the components of the neutral wind, used in producing results shown by the solid lines of Fig. 18, were taken to be zero after 12:00 UT on 27 August and when the zonal electric field and the NRLMSISE-00 neutral temperature and densities are the same as for the solid lines.

It follows from the model calculations that before sunrise on 28 August the meridional wind in both hemispheres is equatorward, with greater magnitude in the Northern Hemisphere. In the Northern Hemisphere, the stronger equatorward wind gives rise to the F-layer being raised to altitudes of lower $O^+(^4S)$ ion loss rate. As a result, the F-layer decays more slowly in the Northern Hemisphere than in the Southern Hemisphere (see the solid line in the panel (c) of Fig. 18). However, the comparison between the solid and dotted lines in the panel (d) of Fig. 18 shows that the change in the magnitude of the morning electron peak caused by the meridional wind is less than about 350° K from about $-30°$ to about 27° geomagnetic longitude, i.e. this change in the electron tem-

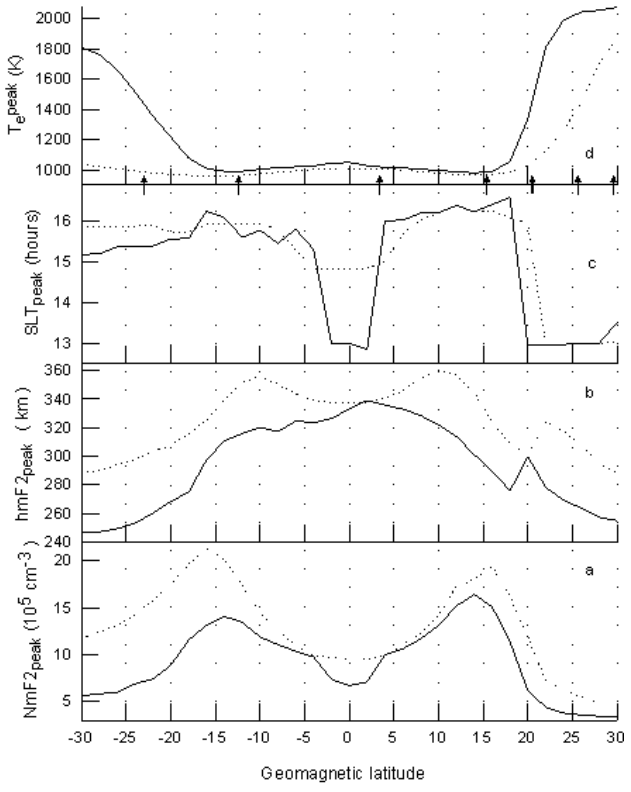

Fig. 19. The latitude dependence of the afternoon electron temperature peak (panel (d)), T_e^{peak}, the time of the evening electron temperature peak appearance (panel (c)), SLT_{peak}, the value of the $F2$ peak layer density at SLT_{peak} (panel (a)), $NmF2_{peak}$, and the $F2$ peak layer altitude at SLT_{peak} (panel (b)), $hmF2_{peak}$, on 25 August 1987. The results shown by the solid lines were calculated by the model with the corrected zonal electric field given by crosses in Fig. 1, the corrected HWW90 wind, and the corrected NRLMSISE-00 neutral temperature and densities. The dotted lines show the results produced by the model with the same value of the zonal electric field as for the solid lines, zero neutral wind, and the NRLMSISE-00 neutral temperature and densities with the same corrections as for the solid lines. Arrows at the top mark the locations of the Darwin, Vanimo, Manila, Okinawa, Yamagawa, Kokubunji, and Akita sounders at $-23.0°$, $-12.4°$, $3.4°$, $15.4°$, $29.6°$, $20.5°$, $25.6°$, and $29.6°$ geomagnetic latitudes, respectively.

perature is not very significant. It means that differences in thermospheric composition between the northern and southern geomagnetic hemispheres are also responsible for a part of the variations in a magnitude of a morning electron temperature peak at $hmF2$ through changes in the production and cooling rates of thermal electrons during a morning time period.

There are disturbances in thermospheric composition and neutral temperature during the main and recovery phases of the geomagnetic storm on 25–27 August, and these disturbances affect the electron temperature through changes in the production and cooling rates of thermal electrons. As a result, we conclude that the main reasons for an appearance, magnitude variations, latitude variations, and a disappearance of the morning electron temperature peaks during 25–27 August are variations in the zonal electric field, thermospheric composition, neutral temperature, and meridian neutral wind.

Figure 19 shows the latitude dependence of the afternoon electron temperature peak (panel (d)), T_e^{peak}, the time of the electron temperature peak appearance (panel (c)), SLT_{peak}, the value of the $F2$ peak layer density at SLT_{peak} (panel (a)), $NmF2_{peak}$, and the $F2$ peak layer altitude at SLT_{peak} (panel (b)), $hmF2_{peak}$, on 25 August 1987. The solid lines show the results from the model with the corrected zonal electric field given by crosses in Fig. 1, the corrected HWW90 wind, and the corrected NRLMSISE-00 neutral temperature and atomic oxygen density. The dotted lines show the results produced by the model with the same value of the zonal electric field as for the solid lines, zero neutral wind, and the NRLMSISE-00 neutral temperature and densities with the same corrections as for the solid lines.

The present study has shown that the magnitude of the evening electron temperature peak and its time location are decreased with the lowering of the geomagnetic latitude, and the evening electron temperature peak disappears from about $-4°$ to about $4°$ geomagnetic latitude and above about $18°$ geomagnetic latitude on 25 August 1987, where an afternoon daytime electron temperature peak exists only. We found that the magnitude of the evening electron temperature peak is decreased, and this peak disappears from about $-6°$ to about $6°$ geomagnetic latitude and above about $20°$ geomagnetic latitude on 25 August 1987, if zero wind is used in the calculations by the model with the corrected zonal electric field given by crosses in Fig. 1, and the corrected NRLMSISE-00 neutral temperature and densities.

The plasma drift along magnetic field lines due to the neutral wind can increase or decrease in $hmF2$, leading to the decrease or increase in the loss rate of $O^+(^4S)$ ions at $hmF2$, causing an increase or a decrease in $NmF2$, and, as a result, leading to a disappearance or an appearance of the evening peak in T_e, respectively. We conclude from the model calculations that a wind, which is poleward by day at low solar activity, forces the $F2$ layer to descend to low altitudes of heavy chemical $O^+(^4S)$ ion losses, reducing the electron density to low values before sunset. A decrease in the production rate of O^+ ions by solar radiation caused by a solar zenith angle increase results in a $NmF2$ decrease with the passage of time during an evening time period. As follows from the model calculations with zero wind, an evening electron temperature peak can be created by this evening electron density decrease. As a result of the poleward wind, the evening $NmF2$ decrease with time becomes strong, producing a strongly pronounced decrease in the thermal electron cooling rate and the increase in the magnitude of the resulting evening electron temperature peak. This result is in agreement with the conclusion of Otsuka et al. (1998), who found that the occurrence and strength of the evening peaks in T_e over the MU radar are determined by the meridional wind under magnetically quiet conditions during 1986–1995. The decrease in the absolute value of the geomagnetic latitude

leads to the weakening of the effect of the plasma drift due to the neutral wind on the electron density. This explains the calculated latitude variations in the strength of the evening peak in the electron temperature on 25 August.

Storm-time variations in thermospheric composition and the neutral temperature during the main and recovery phases of the geomagnetic storm on 25–27 August can affect the electron temperature through changes in the production and cooling rates of thermal electrons, while disturbances in the zonal electric field can change the electron density, leading to changes in the electron temperature. As a result, we conclude that storm-time variations in the meridian neutral wind, thermospheric composition, neutral temperature, and zonal electric field cause the difference in an appearance, magnitude variations, latitude variations, and a disappearance of the evening electron temperature peaks between the evening peak on 25 August and those on 26–27 August.

5 Conclusions

We have presented a comparison between the modeled and experimental $NmF2$ and $hmF2$ at the anomaly crest and close to the geomagnetic equator simultaneously by the Akita, Kokubunji, Yamagawa, Okinawa, Manila, Vanimo, and Darwin ionospheric sounders and by the MU radar during the 25–27 August 1987 geomagnetically storm-time period at low solar activity near approximately the same geomagnetic meridian of 201°. A comparison between the electron and ion temperatures measured by the MU radar and those produced by the model of the ionosphere and plasmasphere is presented for 25–27 August 1987. The model reproduces major features of the data.

It is shown that the dependence of $NmF2$ on [N_2] and [O_2] is weaker than the dependence of $NmF2$ on [O] by day, close to the geomagnetic equator, i.e. $NmF2$ is not proportional to [O]/[N_2] or to [O]/[O_2] in the low-latitude daytime ionosphere, close to the geomagnetic equator.

The similarity of the equatorial anomaly on 25 and 27 August is found. The geomagnetic latitude variations in the electron density calculated for 26 August 1987 (the recovery phase of the geomagnetic storm) differ significantly from those calculated for 25 August 1987 (before SSC and during the main phase of the geomagnetic storm) and for 27 August 1987 (after the geomagnetic storm). The equatorial plasma fountain undergoes significant inhibition on 26 August. During 25 and 27 August, the model produces the onset of the equatorial anomaly crest formation near 01:00-01:30 UT and the crests disappear close to 14:00 UT, while a geomagnetic latitude electron density profile with two equatorial anomaly crests is distinguished from 01:00 UT to 04:00 UT on 26 August.

There is an asymmetry in $hmF2$ and $NmF2$ between the northern and southern geomagnetic hemispheres on 25 and 27 August. This asymmetry in $NmF2$ is much stronger on 26 August than that on 25 or 27 August. It is found that the asymmetry in the neutral wind determines most of the asymmetry in $hmF2$ and $NmF2$ on 25 and 27 August from about 01:00–01:30 UT to about 14:00 UT when the equatorial anomaly exists in the ionosphere, while both asymmetries in neutral winds and in neutral temperature and densities relative to the geomagnetic equator are responsible for the north-south asymmetry in $NmF2$ and $hmF2$ on 26 August.

It is shown that the differences between the disturbed and quiet zonal electric fields, which are most pronounced from 14:00–16:00 UT to 20:00–23:00 UT, cause the corresponding noticeable variations in the calculated $NmF2$ from about 16:00-17:00 UT to about 20:00–22:00 UT.

We found that, close to the geomagnetic equator, the $hmF2$ and $NmF2$ variations caused by neutral winds, are stronger on 26 August than those on 25 and 27 August from 02:00 UT to 11:00 UT. The neutral winds inhibit the development of the equatorial anomaly, leading to a decrease in the crest-to-trough ratio. It is shown that the major storm effect, namely, the suppression of the equatorial anomaly on 26 August, is not due to a reduction in the plasma drift perpendicular to the geomagnetic field direction (i.e. it is not caused by a reduction in the zonal electric field), but is due to the action of storm-time changes in neutral winds and densities on the plasma fountain process.

It is shown that, in the plane of the geomagnetic meridian at the geomagnetic longitude of 201°, the increase in the loss rate of $O^+(^4S)$ ions, due to the vibrational excited N_2 and O_2, causes the maximum decrease in the calculated $NmF2$ by a factor of 1.12, 1.26, and 1.13 and the maximum change in the calculated $hmF2$ of 4, 11, and 4 km in the low-latitude ionosphere between $-30°$ and $+30°$ of the geomagnetic latitude at low solar activity on 25, 26, and 27 August, respectively.

The diurnal solar local time variations of T_e are characterized by morning peaks above the Darwin Vanimo, Manila, and Okinawa ionosonde stations during 26–28 August, and above the Akita ionosonde station and the MU radar on 28 August, and by feebly marked morning electron temperature peaks over the Yamagawa ionosonde station on 27 and 28 August. The model produces evening peaks in the diurnal solar local time electron temperature variations over the MU radar (on 25 August), the Darwin (on 25–27 August), Vanimo (on 26 August), Yamagawa (on 25 and 26 August), and Akita (on 25 and 26 August) ionosonde stations. A broad evening-daytime maximum in the electron temperature is calculated above Manila and Okinawa on 25 August and over Vanimo on 25 and 27 August.

There is a rapid heating of daytime electrons by photoelectrons, and the difference between the electron and ion temperatures is increased after sunrise because nighttime electron densities are less than those by day, and the resulting electron cooling is less than that by day. After the abrupt morning increase, the electron temperature decreases due to the increase in the cooling rate of thermal electrons caused by the increase in the electron density. The magnitude of the morning electron temperature peak at $hmF2$ depends on a value of the morning $NmF2$ which is a function of a minimum value of the nighttime $NmF2$ before sunrise. The nighttime downward $\boldsymbol{E}\times\boldsymbol{B}$ drift causes the decrease in

$NmF2$ before sunrise, and, as a result, part of the increase in the magnitude of the morning peak in the electron temperature is explained by the effects of this drift on the electron density. The nighttime downward $\boldsymbol{E}\times\boldsymbol{B}$ drift becomes more effective in lowering the electron density with lowering geomagnetic latitude, i.e. a decrease in the absolute value of the geomagnetic latitude leads to a decrease in the nighttime electron density before sunrise and a resulting increase in the magnitude of the morning electron temperature peak. It is shown that the change in the magnitude of the morning electron peak caused by the meridional wind is not significant. Differences in the thermospheric composition between the northern and southern geomagnetic hemisphere are also partially responsible for a morning electron temperature peak variations at $hmF2$ through changes in the production and cooling rates of thermal electrons during a morning time period. It is shown that the main reasons for an appearance, magnitude variations, latitude variations, and a disappearance of the morning electron temperature peaks during 25–27 August are variations in the zonal electric field, thermospheric composition, neutral temperature, and meridian neutral wind.

The present study has shown that the magnitude of the evening electron temperature peak and its time location are decreased with lowering the geomagnetic latitude, and the evening electron temperature peak disappears from about -4° to about 4° geomagnetic latitude and above about 18° geomagnetic latitude on 25 August. It is shown that a wind, which is poleward by day at low solar activity, forces the $F2$ layer to descend to low altitudes of heavy chemical $O^+(^4S)$ ion losses, reducing the electron density to low values before sunset. A decrease in the production rate of O^+ ions by solar radiation caused by a solar zenith angle increase results in a $NmF2$ decrease with time during an evening time period. An evening electron temperature peak can be created by this evening electron density decrease. Due to the poleward wind, the evening $NmF2$ decrease with time becomes strong, producing a strongly pronounced decrease in the thermal electron cooling rate and the increase in the magnitude of the resulting evening electron temperature peak. The decrease in the absolute value of the geomagnetic latitude leads to the weakening of the effect of the plasma drift due to the neutral wind on the electron density, leading to the decrease in the magnitude or to a disappearance of the evening peak in the electron temperature. Storm-time variations in thermospheric composition and the neutral temperature during the main and recovery phases of the geomagnetic storm on 25–27 August can affect the electron temperature through changes in the production and cooling rates of thermal electrons, while disturbances in the zonal electric field can change the electron density, leading to changes in the electron temperature. Therefore, storm-time variations in the meridian neutral wind, thermospheric composition, neutral temperature, and zonal electric field cause the difference between 25 August and 26–27 August in an appearance, magnitude and latitude variations, and a disappearance of the evening electron temperature peaks.

Acknowledgements. The authors of the paper acknowledge Prof. B. G. Fejer and Dr. L. Schlerliess for providing us by the Fortran codes of the empirical models of the plasma drift over the geomagnetic equator for quiet and disturbed conditions and by the measurements of the plasma drift over Jicamarca at F-region altitudes. We thank Prof. B. G. Fejer for a discussion of preliminary results. The MU radar belongs to and is operated by RASC. Hourly critical frequencies $foF2$, foE and maximum usable frequency parameters M(3000)$F2$ data from the ionospheric sounder stations were provided by the National Geophysical Data Center at Boulder, Colorado. A. V. Pavlov was supported by grant 02-05-64204 from the Russian Foundation for Basic Research. The authors would like to thank referees for their comments on the paper, which have assisted in improving the final version.

Topical Editor M. Lester thanks J. H. Sobral and another referee for their help in evaluating this paper.

References

Abdu, M. A., Sobral, J. H. A., de Paula, E. R., and Batista, I. S.: Magnetospheric disturbance effects on the Equatorial Ionization Anomaly (EIA) - an overview, J. Atmos. Terr. Phys., 53, 757–771, 1991.

Abdu, M. A.: Major phenomena of the equatorial ionosphere-thermosphere system under disturbed conditions, J. Atmos. Terr. Phys., 59, 1505–1519, 1997.

Abdu, M. A.: Outstanding problems in the equatorial ionosphere-thermosphere electrodynamics relevant to spread F, J. Atmos. Terr. Phys., 63, 869–884, 2001.

Anderson, D. N.: Modeling the ambient, low-latitude F-region ionosphere - A review, J. Atmos. Terr. Phys., 43, 753–762, 1981.

Aponte, N., González, S. A., Kelley, M. C., Tepley, C. A., Pi, X., and Iijima, B.: Advection of the equatorial anomaly over Arecibo by small-storm related disturbance dynamo electric fields, Geophys. Res. Lett., 27, 2833–2836, 2000.

Balan, N. and Bailey, G. J.: Equatorial plasma fountain and its effects: Possibility of an additional layer, J. Geophys. Res., 100, 21 421–21 432, 1995.

Balan, N., Bailey, G. J., Abdu, M. A., Oyama, K. I., Richards, P. G., MacDougall, J., and Batista, I. S.: Equatorial plasma fountain and its effects over three locations: Evidence for an additional layer, the F_3 layer, J. Geophys. Res., 102, 2047–2056, 1997a.

Balan, N., Otsuka, Y., and Fukao, S.: New aspects in the annual variation of the ionosphere observed by the MU radar, Geophys. Res. Letters, 24, 2287–2290, 1997b.

Bailey, G. J. and Balan, N.: A low-latitude ionosphere-plasmasphere model, in Handbook of Ionospheric Models, edited by R.W. Schunk, pp. 173–206, Utah State Univ., Logan, Utah, 1996.

Blanc, M. and Richmond, A.D.: The ionospheric disturbance dynamo, J. Geophys. Res., 85, 1669–1686, 1980.

Buonsanto, M. J.: Ionospheric storms—a review, Space Science Reviews, 88, 563–601, 1999.

Buonsanto, M. J., González, S. A., Pi, X., Ruohoniemi, J. M., Sulzer, M. P., Swartz, W. E., Thayer, J. P., and Yuan, D. N.: Radar chain study of the May, 1995 storm, J. Atmos. Sol. Terr. Phys., 61, 233–248, 1999.

Burge, J. D., Eccles, D., King, J. W., and Ruster, R.: The effects of thermospheric winds on the ionosphere at low and middle latitudes during magnetic disturbances, J. Atmos. Terr. Phys., 35, 617–623, 1973.

Chandra, S. and Spencer, N.W.: Thermospheric storms and related ionospheric effects, J. Geophys. Res., 81, 5018–5026, 1976.

Dudeney, J. R.: The accuracy of simple methods for determining the height of the maximum electron concentration of the $F2$-layer from scaled ionospheric characteristics, J. Atmos. Terr. Phys., 45, 629–640, 1983.

Emmert, J. T., Fejer, B. G., Fesen, C. G., Shepherd, G. G., and Solheim, B. H.: Climatology of middle- and low-latitude daytime F-region disturbance neutral winds measured by Wind Imaging Interferometer (WINDII), J. Geophys. Res., 106, 24 701–24 712, 2001.

Fejer, B. G.: F-region plasma drifts over Arecibo - Solar cycle, seasonal, and magnetic activity effects, J. Geophys. Res., 98, 13 645–13 652, 1993.

Fejer, B. G.: Low latitude storm-time ionospheric electrodynamics, J. Atmos. Sol. Terr. Phys., 64, 1401–1408, 2002.

Fejer, B. G., and Scherliess, L.: Empirical models of storm-time equatorial zonal electric fields, J. Geophys. Res., 102, 24 047-24 056, 1997.

Fejer, B. G., and Scherliess, L.: Empirical models of storm-time equatorial zonal electric fields, J. Geophys. Res., 102, 24 047–24 056, 1997.

Fejer, B. G., Emmert, J. T., and Sipler, D. P.: Climatology and storm-time dependence of nighttime thermospheric neutral winds over Millstone Hill, J. Geophys. Res.,107, pp. SIA 3–1, CiteID 1052, DOI 10.1029/2001JA000300, 2002.

Fesen, C. G., Crowley, G., and R. G. Roble,:Ionospheric effects at low-latitudes during the March 22, 1979, geomagnetic storm, J. Geophys. Res., 94, 5405–5417, 1989.

Fuller-Rowell, T. J., Millward, G. H., Richmond, A. D., and Codrescu, M. V.: Storm-time changes in the upper atmosphere at low-latitudes, J. Atmos. Sol. Terr. Phys., 64, 1383–1391, 2002.

Fukao, S., Sato, T., Tsuda, T., Yamamoto, M., Yamanaka, M. D., and Kato, S.: MU radar: new capabilities and system calibrations, Radio Sci., 25, 477–485, 1990.

Gonzales, C. A., Behnke, R. A., Kelley, M. C., Vickrey, J. F., Wand, R., and Holt, J.: On the longitudinal variations of the ionospheric electric field during magnetospheric disturbances, J. Geophys. Res., 88, 9135–9144, 1983.

Gonzalez, W. D., and Tsurutani, B. T.: Criteria of interplanetary parameters causing intense magnetic storms ($D_{st} < -100$ nT), Planet. Space Sci., 35, 1101–1109, 1987.

Hedin, A. E., Spencer, N. W., Biondi, M. A., Burnside, R. G., Hernandez, G., and Johnson, R. M.: Revised global model of thermosphere winds using satellite and ground-based observations, J. Geophys.Res., 96, 7657–7681, 1991.

Kawamura, S., Otsuka, Y, Zhang, S.-R., Fukao, S., and Oliver, W. L.: A climatology of MU radar observations of thermospheric winds, J. Geophys. Res., 105, 12 777–12 788, 2000.

Kawamura, S.: A study of wind variations and their effects on the mid latitude ionosphere and thermosphere based on the MU radar observations, PhD Thesis, Radio Science Center for Space and Atmosphere Kyoto University, Japan, 2003.

Kelley, M. C., Fejer, B. G., and Gonzales, C. A.: An explanation for anomalous equatorial ionospheric electric fields associated with a northward turning of the interplanetary magnetic field, Geophys. Res. Lett., 6, 301–304, 1979.

Lobzin, V. V. and Pavlov, A. V.: G condition in the $F2$ region peak electron density: a statistical study, Ann. Geophys., 20, 523–538, 2002.

McClure, J. P.: Diurnal variation of neutral and charged particle teperatures in the equatorial F-region, J. Geophys. Res., 74, 279–291, 1969.

Moffett, R. J.: The Equatorial Anomaly in the Electron Distribution of the Terrestrial F-Region, Fundamentals of Cosmic Physics, 4, 313–391, 1979.

Oliver, W. L., Fukao, S., Sato, T., Tsuda, T., Kato, S., Kimura, I., Ito, I., Saryou, T., and Araki, T.: Ionospheric incoherent scatter measurements with the Middle and Upper Atmosphere Radar: Observations during the large magnetic storm of 6–8 February, 1986, J. Geophys. Res., 93, 14 649–14 655, 1988.

Oliver, W. L., Fukao, S., Takami, T., Tsuda, T., and Kato, S.: Four-beam measurements of ionospheric structure with the MU radar during the low-latitude auroral event of 20-23 October 1989, Geophys. Res. Lett., 18, 1975–1978, 1991.

Otsuka, Y., Kawamura, S., Balan, N., Fukao, S., and Bailey, G. J.: Plasma temperature variations in the ionosphere over the middle and upper atmosphere radar, J. Geophys. Res., 103, 20 705–20 713, 1998.

Pavlov, A. V.: New electron energy transfer rates for vibrational excitation of N_2, Ann. Geophys., 16, 176–182, 1998a.

Pavlov, A. V.: New electron energy transfer and cooling rates by excitation of O_2, Ann. Geophys., 16, 1007–1013, 1998b.

Pavlov, A. V.: New method in computer simulations of electron and ion densities and temperatures in the plasmasphere and low-latitude ionosphere, Ann. Geophys., 21, 1601–1628, 2003.

Pavlov, A. V. and Berrington, K. A.: Cooling rate of thermal electrons by electron impact excitation of fine structure levels of atomic oxygen, Ann. Geophys., 17, 919–924, 1999.

Pavlov, A. V., Fukao, S., and Kawamura, S.: Comparison of the measured and modeled electron densities and electron and ion temperatures in the low-latitude ionosphere during 19-21 March 1988, Ann. Geophys., 22, 2747–2763, 2004.

Picone, J. M., Hedin, A. E., Drob, D. P., and Aikin, A. C.: NRLMSISE-00 empirical model of the atmosphere: statistical comparisons and scientific issues, J. Geophys. Res., 107(A12), 1468, doi:10.1029/2002JA009430, 2002.

Pincheira, X. T., Abdu, M. A., Batista, I. S., and Richards, P. G.: An investigation of ionospheric responses, and disturbance thermospheric winds, during magnetic storms over South American sector, J. Geophys. Res., 107(A11), 1379, doi: 10.1029/2001JA000263, 2002.

Reddy, C. A., Fukao, S., Takami, T., Yamamoto, M., Tsuda, T., Nakamura, T., and Kato, S.: A MU radar-based study of mid-latitude F-region response to a geomagnetic disturbance, J. Geophys. Res., 95, 21 077–21 094, 1990.

Rees, M. H.: Physics and chemistry of the upper atmosphere, Cambridge and New York, Cambridge University Press, 1989.

Richards, P. G., Fennelly, J. A., and Torr, D. G.: EUVAC : A solar EUV flux model for aeronomical calculations, J. Geophys. Res., 99, 8981–8992, 1994 (Correction in J. Geophys. Res., 99, 13 283, 1994.)

Rishbeth, H., and Garriot, O.: Introduction to ionospheric physics, New York, Academic Press, 1969.

Rishbeth, H.: F-region storms and thermospheric circulations, J. Atmos. Terr. Phys., 37, 1055–1064, 1975.

Rishbeth, H.: The equatorial F-layer: progress and puzzles, Ann. Geophys., 18, 730–739, 2000.

Rishbeth, H., and Fukao, S.: A review of MU radar observations of the thermosphere and ionosphere, J. Geomagn. Geoelectr., 47, 621–637, 1995.

Sato, T., Fukao, S., Tsuda, T., Ito, A., and Oliver, W. L.: Ionospheric incoherent scatter measurements with the middle and upper atmosphere radar - Techniques and capability, Radio Science, 24,

85–98, 1989.

Sastri, J. H., Jyoti, N., Somayajulu, V. V., Chandra, H., and Devasia, C. V.: Ionospheric storm of early November 1993 in the Indian equatorial region, J. Geophys. Res., 105, 18 443–18 456, 2000.

Scherliess, L., and Fejer, B.G.: Radar and satellite global equatorial F-region vertical drift model, J. Geophys. Res., 104, 6829–6842, 1999.

Senior, C. and Blanc, M.: On the control of magnetospheric convection by the spatial distribution of ionospheric conductivities, J. Geophys. Res., 89, 261–284, 1984.

Shimazaki, T.: World-wide variations in the height of the maximum electron density of the ionospheric $F2$ layer, J. Radio Res. Labs. Japan, 2(7), 85–97, 1955.

Souza, J. R., Abdu, M. A., Batista, I. S. Bailey, G. J.: Determination of vertical plasma drift and meridional wind using the Sheffield University Plasmasphere Ionosphere Model and ionospheric data at equatorial and low-latitudes in Brazil: Summer solar minimum and maximum conditions, J. Geophys. Res., 105, 12 813–12 821, 2000.

Spiro, R. W., Wolf, R. A., and Fejer, B. G.: Penetrating of high-latitude-electric-field effects to low-latitudes during SUNDIAL 1984, Ann. Geophys., 6, 39–49, 1988.

Takami, T., Oliver, W. L., Richmond, A. D., and Fukao, S.: Ionospheric drift similarities at magnetic conjugate and nonconjugate locations, J. Geophys. Res., 101, 15 73–15 782, 1996.

Titheridge, J. E.: Winds in the ionosphere - a review, J. Atmos. Terr. Phys., 57, 1681–1714, 1995.

Vasyliunas, V. M.: Theoretical models of magnetic field line merging. I ., Rev. Geophys. Space Phys., 13, 303–336, 1975.

Walker, G. O.: Longitudinal structure of the F-region equatorial anomaly - A review, J. Atmos. Terr. Phys., 43, 763–774, 1981.